NASA/CR—2020-220453

Cold-Flow Model Tests to Determine Static Performance of a NASA One-Sided Ejector Nozzle System

Alan S. Estenson and Timothy J. McDonald
Aero Systems Engineering Inc., Plymouth, Minnesota

January 2020

NASA STI Program . . . in Profile

Since its founding, NASA has been dedicated to the advancement of aeronautics and space science. The NASA Scientific and Technical Information (STI) Program plays a key part in helping NASA maintain this important role.

The NASA STI Program operates under the auspices of the Agency Chief Information Officer. It collects, organizes, provides for archiving, and disseminates NASA's STI. The NASA STI Program provides access to the NASA Technical Report Server—Registered (NTRS Reg) and NASA Technical Report Server—Public (NTRS) thus providing one of the largest collections of aeronautical and space science STI in the world. Results are published in both non-NASA channels and by NASA in the NASA STI Report Series, which includes the following report types:

- TECHNICAL PUBLICATION. Reports of completed research or a major significant phase of research that present the results of NASA programs and include extensive data or theoretical analysis. Includes compilations of significant scientific and technical data and information deemed to be of continuing reference value. NASA counter-part of peer-reviewed formal professional papers, but has less stringent limitations on manuscript length and extent of graphic presentations.

- TECHNICAL MEMORANDUM. Scientific and technical findings that are preliminary or of specialized interest, e.g., "quick-release" reports, working papers, and bibliographies that contain minimal annotation. Does not contain extensive analysis.

- CONTRACTOR REPORT. Scientific and technical findings by NASA-sponsored contractors and grantees.

- CONFERENCE PUBLICATION. Collected papers from scientific and technical conferences, symposia, seminars, or other meetings sponsored or co-sponsored by NASA.

- SPECIAL PUBLICATION. Scientific, technical, or historical information from NASA programs, projects, and missions, often concerned with subjects having substantial public interest.

- TECHNICAL TRANSLATION. English-language translations of foreign scientific and technical material pertinent to NASA's mission.

For more information about the NASA STI program, see the following:

- Access the NASA STI program home page at http://www.sti.nasa.gov

- E-mail your question to help@sti.nasa.gov

- Fax your question to the NASA STI Information Desk at 757-864-6500

- Telephone the NASA STI Information Desk at 757-864-9658

- Write to:
  NASA STI Program
  Mail Stop 148
  NASA Langley Research Center
  Hampton, VA 23681-2199

NASA/CR—2020-220453

Cold-Flow Model Tests to Determine Static Performance of a NASA One-Sided Ejector Nozzle System

Alan S. Estenson and Timothy J. McDonald
Aero Systems Engineering Inc., Plymouth, Minnesota

Prepared under Contract 80NSSC18P3017

National Aeronautics and
Space Administration

Glenn Research Center
Cleveland, Ohio 44135

January 2020

This work was sponsored by the Advanced Air Vehicle Program
at the NASA Glenn Research Center

Level of Review: This material has been technically reviewed by expert reviewer(s).

Available from

NASA STI Program
Mail Stop 148
NASA Langley Research Center
Hampton, VA 23681-2199

National Technical Information Service
5285 Port Royal Road
Springfield, VA 22161
703-605-6000

This report is available in electronic form at http://www.sti.nasa.gov/ and http://ntrs.nasa.gov/

TABLE OF CONTENTS

LIST OF FIGURES

FOREWORD

This report was prepared by FluiDyne Aerotest Laboratory of AeroSystems Engineering, Inc., Plymouth, MN for NASA Glenn Research Center (GRC), Cleveland, OH, under NASA Shared Services purchase order 80NSSC18P3017. It was originally prepared as Aerosystems Fluidyne Aerotest Laboratory Report number L18333. It documents thrust data and related experimental procedures for a one-sided ejector system that was developed and tested earlier at GRC.

Mr. Raymond S. Castner of Inlets and Nozzles Branch served as the NASA monitor for the project. Other cognizant personnel at GRC were Dr. Khairul Zaman of the same Branch and Dr. James Bridges of the Acoustics Branch. ASE FluDyne's lead engineers were Kevin L. Mikkelsen and Alan S. Estenson.

The project was supported by NASA's Commercial Supersonics Technology Project (CST). Support from Mr. David Friedlander of Inlets and Nozzles Branch and Dr. Amy Fagan of Optics and Photonics Branch during the course of this project are also gratefully acknowledged.

SUMMARY

This report presents the results of cold-flow model tests to determine the static performance of multiple configurations of a NASA one-sided ejector nozzle system. The existing ejector nozzle system hardware was provided by NASA and was previously used for acoustic tests. A new facility adapter duct and ejector box support brackets were designed and fabricated by the FluiDyne Aerotest Laboratory of Aero Systems Engineering, Inc. The tests were performed in the Channel 8 static thrust stand at ASE's FluiDyne Aerotest Laboratory in Plymouth, Minnesota.

Facility checkout tests were made using a standard American Society of Mechanical Engineers (ASME) long-radius metering nozzle. These tests demonstrated facility data accuracy at flow conditions similar to the model tests.

Channel 8 static tests included 40 ASME nozzle facility checkout tests and 24 model tests (plus an additional 1 at no charge). The model nozzle pressure ratio varied from 1.4 to 3.0.

Test results include: thrust coefficients, thrust vector angles and location, nozzle discharge coefficients, charging station total and static pressures, and model static pressure distributions (in the Data Appendix).

DEFINITION OF SYMBOLS

a	Speed of sound
A	Cross-section area, in^2
A*	Sonic throat area, in^2
b	Real-gas ideal thrust function correction, dimensionless
B_j	Balance readout, millivolts
C_D	Discharge coefficient, dimensionless
C_T	Thrust coefficient, dimensionless
d	Diameter, inches
g	Acceleration of gravity, 32.174 ft/sec^2
H_r	Resultant thrust, lb_f
H_x	Axial thrust, lb_f
H_y	Vertical thrust, lb_f
K	Real-gas mass flow function, (lb_m °$R^{1/2}$)/(lb_f sec)
L_{ref}	Axial distance from the balance vertical bridge V3 to the model reference plane at exit of the fan nozzle. (L_{ref} = 32.25 inches to exit of ejector box)
L_x	Axial distance to the intersection of the resultant thrust vector with the model centerline, measured from the model reference plane, positive downstream of the reference plane, inches
L_y	Vertical displacement of resultant thrust vector at the reference plane, measured from nozzle centerline to the intersection of the thrust vector and the reference plane, positive upward, inches
m	Mass flow rate, slugs/second
M	Mach number, dimensionless
MO	Pitching moment about the intersection of the reference plane and the model centerline, positive clockwise with flow left to right, (=$L_x H_y$), inlb_f
P	Pressure, static unless otherwise specified by subscript, psia
r	Radius from centerline, inches
Δr	see L_y inches
R	Gas constant, 1716.32 ft^2/sec^2°R

R_N	Reynolds number, dimensionless
T	Temperature, °R (unless stated as °F)
v	Velocity, ft/sec
W	Mass flow rate, lb_m/sec
W_x,W_y	Dead-weight calibration loads, lb_f
y	Distance from wall
α	Thrust vector angle, degrees
γ	Ratio of specific heats, dimensionless
δ	Boundary layer thickness
θ	Meridian angle measured clockwise from top looking upstream, degrees
λ	Pressure ratio, P_t/P_a, dimensionless
ρ	Density, slugs/ft^3
Σ	Summation
Δ	Incremental quantity
τ	Temperature ratio, T_{t8}/T_{t7}, dimensionless
η	Temperature difference ratio, $(T - T_{t7})/(T_{t8} - T_{t7})$, dimensionless

Subscripts

a	Ambient
e	Exit
i	Ideal
i,j	Counter for summations
r	Resultant
t	Total conditions
w	Wall
x	Axial component
y	Vertical component
∞	Freestream
1,2,...	See Figures 3 and 7

Superscript

*	Sonic condition, M = 1

1.0 INTRODUCTION

This cold flow model study investigated the static performance of a NASA one-sided ejector nozzle system. The existing nozzle and ejector box hardware were provided by NASA and were previously tested at NASA for acoustics. A facility adapter and ejector box support system were designed and fabricated by ASE for these tests. The tests were conducted at Aero Systems Engineering's FluiDyne Aerotest Laboratory located in Plymouth, Minnesota. Tests were conducted in the Channel 8 static thrust stand and exhausted directly to atmosphere.

The test program was defined by NASA test specifications. NASA technical liaisons for these tests included Dr. Khairul Zaman, Mr. Raymond Castner, Dr. James Bridges, and Mr. David Friedlander.

This report describes the test facility, test model, data acquisition and analysis procedures, and presents the test results. Test conditions and major results are tabulated and plotted in Figures 10 - 13. Detailed data and calculations are contained in a separate Appendix. Detailed ASE part drawings are included at the end of this report.

2.0 FACILITY DESCRIPTION

The tests described in this report were performed in the Channel 8 static thrust stand at Aero Systems Engineering's FluiDyne Aerotest Laboratory located in Plymouth, Minnesota.

2.1 Channel 8 Static Thrust Stand

Channel 8 is a cold-flow, high-pressure-ratio, static thrust stand with the ability to exhaust either to atmosphere or into a sealed test cabin connected to a vacuum system or ejector. The general arrangement of Channel 8 is shown in Figures 1, 3 and 7.

The airflow for the test nozzle is obtained from the facility 500-psi dry air storage system. Air is throttled, metered through the Station 1 ASME long-radius metering nozzle, and discharged through the test model either to atmosphere or the facility vacuum system.

The model assembly is supported by a 3-component strain-gage force balance and is isolated from the facility piping by a seal; see schematics in Figures 3 and 7. For the current tests, the model airflow was nominally 70 °F.

For all tests described in this report, the test cabin was in an open configuration as shown in Figure 9a. The model exhausted into the open cabin and diffuser. The diffuser piping system was opened to allow the model flow to exhaust to atmosphere.

Facility instrumentation is provided to calculate the mass flow rates at Station 1 and to calculate the exit thrust produced by the test nozzle; details are described in Section 4. The test data include measurements of axial and vertical balance forces, air mass flow rates, model total and static pressures, and the air temperatures and pressures necessary to calculate the flow rate and forces. Static and total pressures were measured with an Esterline Pressure Systems Inc. (PSI) Netscanner 98RK with Model 9816 multi-ported transducers. Force balance and temperature signals were recorded with a Hewlett-Packard / Agilent 34970a electronic data acquisition system.

2.2 Operational Procedures

The Channel 8 desired nozzle flow was set by regulating the total airflow to obtain the desired pressure ratio to atmosphere, P_{t8}/P_a, in the ASE charging station duct upstream of the model adapter duct.

3.0 MODEL DESCRIPTION

3.1 Model Adapters

Facility adapting hardware as well as flow conditioning and a charging station duct were provided by ASE. The flow conditioning consisted of two perforated plates and five screens. Flow conditioning details are provided in the Data Appendix.

A facility adapter duct (L18333-100) was used to transition from the ASE-provided charging station and flow conditioning duct to the NASA nozzle hardware. This duct was designed and fabricated by ASE.

3.2 Model Components

The nozzle round-to-rectangular transition duct, AR 8:1 rectangular nozzle tip ('NA8Z'), ejector box assembly, plastic plugs for setting the position of the ejector upper plate, and tab strip were provided by NASA. The charging station and flow conditioning were provided by ASE. Support brackets (L18333-101) to attach the ejector nozzle assembly to the primary nozzle assembly were designed and fabricated by ASE. The existing ejector left and right side plates were modified by ASE to allow attachment of these brackets (L18333-102).

Because the existing model components did not incorporate o-ring seals, a variety of sealing methods were utilized. A non-adhesive two-part RTV compound was used to create a seal within the joint between the round-to-rectangular duct and the rectangular nozzle tip. At the joint between the rectangular nozzle tip and the side and bottom plates of the ejector box, an adhesive Loctite 5920 RTV was applied externally to create a seal. (See Figure 9e and the notes on Figure 2 – drawing

L18333-010.) Small gaps between the ejector box side plates and upper surface of the primary nozzle were blocked with foam sealing tape, Figure 9d.

For these model tests, the variations in configuration included the installation of a tab strip onto the nozzle upper surface and changes in position and angle of the ejector box upper plate. The tab strip was attached using two button head screws and Loctite EA E-20NS 2-part epoxy. The heads of the two mounting screws were filled in with red wax. The position and angle of the upper plate was set by installing different combinations of plastic plugs in the ejector box side walls. The plastic plugs that were used in each configuration are documented in Figure 8. For each configuration, the heights of the ejector entry slot and ejector box exit were inspected. These inspection results are documented in Figure 8 and in the separate Data Appendix.

An unused mounting hole in the bottom plate of the ejector box was plugged with a provided countersunk screw and nut. Red wax was used to fill above the screw head and provide a smooth flow surface.

The model assembly is shown in Figure 2 – drawing L18333-010. Model configurations are defined in Figure 8. Photographs of model assemblies and components are shown in Figures 9a-i. Detailed ASE drawings of the test hardware are contained in the last section of this report and on the DVD-ROM.

3.3 Model Instrumentation

The charging station instrumentation for the model (station 8) consisted of two 6-probe area-weighted rakes (P_{t8}) at theta = 100 and 260 degrees. Four associated static pressures (P_{s8}) were located on the outer wall at 45, 135, 225, and 315 degrees. (Theta equals 0 degrees at model top-dead-center and is positive in the clockwise direction when looking upstream.) This charging station was located upstream of the transition adapter duct and nozzle model.

Five static pressure taps were located in a row along the centerline of the ejector box upper plate; they are shown in photographs in Figure 9.

Four tubes were taped into place on the ejector box upper and lower plates such that their open ends were flush with the aft-facing surface. (Figure 9e) These tubes measured “flange” static pressures near the ejector box exit, but they do not provide a true base area static pressure reading. Two additional open tubes were positioned to measure local pressures upstream from the ejector box inlet. (Figure 9c) These measurements are provided for reference purposes; they were not incorporated into the ASE data reduction process.

Instrumentation details are provided on the individual part drawings.

4.0 DATA ANALYSIS PROCEDURES

The following subsections describe the data analysis procedures. Station notations are defined in Figures 3 and 7.

4.1 P_t Definitions

For these tests, an arithmetic mean method was used to determine the ASE charging station total pressure P_{t8}. The individual P_{t8} probes were physically located in equal area weighted positions. This total pressure measurement was located upstream of the transition duct to the nozzle.

For reference, FluiDyne's standard mass-momentum routine is described below. The mass-momentum method was not used for these tests. For flows with nearly-uniform total pressure profiles, the average total pressure may be obtained by simply area-weighting individual probe measurements. For flows with non-uniform total pressure profiles, however, a more accurate measure of the average total pressure is obtained from the mass-momentum method (Reference 1). This method represents a non-uniform flow by average properties that simultaneously satisfy both the mass flow and the momentum of the real flow.

From continuity:

$$PAM \sqrt{\frac{\gamma}{RT}\left(1 + \frac{\gamma - 1}{2}M^2\right)} = \Sigma P_j A_j M_j \sqrt{\frac{\gamma}{RT_j}\left(1 + \frac{\gamma - 1}{2}M_j^2\right)}$$

and from momentum:

$$PA\,(1 + \gamma M^2) = \Sigma P_j A_j\,(1 + \gamma M_j^2)$$

where the individual A_j were determined from the flow path and rake geometry, P_j is assumed to vary linearly between the inner and outer wall, P_{tj} is measured directly, and

$$M_j = \sqrt{\frac{2}{\gamma - 1}\left[\left(\frac{P_t}{P}\right)^{\frac{\gamma - 1}{\gamma}} - 1\right]}$$

If total temperature is assumed constant in the passage, then:

$$\frac{M\sqrt{1 + \frac{\gamma - 1}{2}M^2}}{1 + \gamma M^2} = \frac{\Sigma P_j A_j M_j \sqrt{1 + \frac{\gamma - 1}{2}M_j^2}}{\Sigma P_j A_j \left(1 + \gamma M_j^2\right)}$$

The right side of the above equation is calculated by summation from the measured quantities. Squaring the above equation results in a quadratic (with variable M^2), which is readily solved for a unique value of the effective Mach number, M, satisfying the stated requirements. Knowing the effective Mach number, the effective static pressure, P, is determined from the preceding continuity equation, and finally, the effective total pressure is calculated from:

$$P_t = P\left(1 + \frac{\gamma - 1}{2}M^2\right)^{\frac{\gamma}{\gamma - 1}}$$

4.2 T_t Definitions

T_{t1} was measured with facility Type K thermocouples. For model performance and ASME checkout nozzle tests, T_{t8} was calculated from T_{t1} by subtracting the temperature drop due to adiabatic throttling of flow between the meter station and the ASE charging station. Adiabatic walls were assumed. The temperature drop was calculated from Joule-Thomson throttling values (Reference 2) and typically varied between 1° and 5°F.

4.3 Flow Rates

The total mass flow rate through the test nozzle system was determined with a choked ASME long-radius metering nozzle at Station 1 (see Figures 3 and 7).

$$W_8 = W_1 = \frac{K_1 C_{D1} A_1 P_{t1} \left(A_1^* / A_1 \right)}{\sqrt{T_{t1}}}$$

The critical flow factor, K, was calculated as a function of total pressure and total temperature. The equation for K, applicable to the range of P_t and T_t normally encountered in the present test facility, was obtained from Reference 3.

$$K = 0.53160 + \left(P_t + 16.9\right)\left(1.581 - 0.00834\left(T_t - 520\right)\right) x\,10^{-5}$$

where T_t is in °R and P_t is in units of psia.

Throat Reynolds Number at Station 1 was calculated using the following equation from Reference 4.

$$R_N = 1.50994\,x\,10^7 \; \frac{P_t\; M\; d \left[T_t \left(1 + 0.2\, M^2\right)^{-1} + 198.6 \right]}{T_t^{\,2} \left(1 + 0.2\, M^2\right)^{1.5}}$$

where all parameters pertain to the desired station.

The meter discharge coefficient, C_{D1}, was calculated as a function of throat Reynolds number using a semi-empirical equation (Reference 6):

Laminar: $R_{N1} < 500{,}000$:

$$C_{D1} = 1 - 6.92 R_{N1}^{-0.5}$$

Transitional: $500{,}000 < R_{N1} < 2{,}000{,}000$:

Perform linear interpolation based on value of R_{N1} between the laminar and turbulent curves.

Turbulent: $R_{N1} > 2{,}000{,}000$:

$$C_{D1} = 1 - 0.184 R_{N1}^{-0.2}$$

For these tests, the values of R_{N1} ranged from approximately 2,100,000 to 5,000,000.

A_1, the meter geometric throat area, was 0.7811-in^2. Meter pressure, P_{t_1}, was measured with the PSI system. T_{t_1} was measured using shielded type K (chromel-alumel) thermocouple probes. All electrical outputs were measured and recorded with a digital data acquisition system.

A^*/A is the isentropic area ratio calculated from the Mach Number at the meter throat. For all test conditions in this calibration, the flow meter was choked, $A^*/A=1$. If the Station 1 flow meter unchoked, A^*/A would be calculated using equations valid for $\gamma = 1.4$.

$$A^*/A = 3.86393\lambda^{-0.71429}\sqrt{1-\lambda^{-0.28571}}, \text{ for } \lambda < 1.8929$$

and

$$A^*/A = 1, \text{ for } \lambda \geq 1.8929,$$

where λ equals the meter total pressure P_{t1} divided by measured throat static pressure, P_2.

Calculated flow rates (lb_m/sec) for these model tests were in the range:

$$1.5 < W_8 < 3.4$$

4.4 Discharge Coefficients

Discharge coefficients were calculated for Channel 8 performance tests. Discharge coefficient is defined as the ratio of the actual flow rate through a nozzle to the ideal isentropic flow rate at the overall nozzle pressure ratio. Overall nozzle pressure ratios are defined as $\lambda_8 = P_{t8}/P_a$. In a static thrust stand, P_a is either atmospheric pressure or test chamber pressure. Because these tests were run with the test cabin open, P_a was the ambient atmospheric pressure in the test facility. The nozzle discharge coefficient is then

$$C_{D8} = W_8/W_{8_i}$$

where

$$W_{8_i} = P_{t_8} A_8 K_8 (A^*/A)_8 / \sqrt{T_{t_8}}$$

P_{t8} and T_{t8}, were defined in Sections 4.1 and 4.2. K_8 was evaluated using a previous equation, as functions of P_{t8} and $T_{t8.}$

The flow area for the nozzle, A_8, was 3.54 in^2. This area was specified by NASA.

For the ASME checkout nozzle tests, the throat area of the 2.25-inch diameter nozzle was A_8 = 3.9729 in^2.

A*/A, the isentropic area ratio, is used to correct the ideal flow rate when the nozzle is unchoked. A*/A for cold flow was calculated using equations valid for $\gamma = 1.4$, obtained from Reference 4.

$$A^*/A = 3.86393\ \lambda^{-0.71429}\sqrt{1-\lambda^{-0.28571}}\ \text{ for } \lambda < 1.8929$$

and

$$A^*/A = 1 \text{ for } \lambda \geq 1.8929.$$

4.5 Thrust Measurement

Model thrust is measured by a force balance system with a control volume approach.

The static axial thrust of an exhaust nozzle is defined as the axial exit momentum of the exhaust flow, plus the excess of exit pressure over ambient pressure times the exit area.

$$H_x = mv_{ex} + (P_e - P_a)\ A_{ex} = \text{axial thrust}$$

The vertical thrust, H_y, was obtained from the vertical force balances. H_y is defined positive downward.

$$H_y = \text{vertical thrust, downward.}$$

The resultant thrust, H_r, was calculated as the vector sum of the axial thrust, H_x, and vertical thrust, H_y. The resultant thrust vector angle relative to the facility centerline was determined as:

$$\alpha = \tan^{-1}\frac{H_y}{H_x}.$$

Referring to Figures 3 and 7, the location of the thrust vector is defined by L_x, the axial distance from the reference plane to the intersection of the resultant thrust vector with the facility centerline. L_x is defined positive downstream of the reference plane. L_x is found by summation of moments.

L_y is the vertical distance to the intersection of the resultant thrust vector with the reference plane, measured positive upward from the model centerline, and is calculated from L_x and α. The reference plane was chosen as the exit plane of the ejector box. Pitching moment about the reference point (model centerline at the reference plane) is calculated as $MO = H_y L_x$. MO is defined positive clockwise with flow from left to right.

The model size was determined by the existing NASA hardware and was small for ASE's force measurement system. However, thrust measurements were acceptable during these tests.

4.6 Static Thrust Coefficients

Thrust coefficient is defined as the ratio of the measured nozzle thrust to the ideal thrust of the duct flow (expanded isentropically from P_{t8} to P_a). In Channel 8, thrust coefficients are calculated for the axial and vertical thrust components, and for the resultant thrust vector (in vertical plane):

$$C_{T_x} = \frac{H_x}{m_8 v_{i8}} \qquad C_{T_y} = \frac{H_y}{m_8 v_{i8}} \qquad C_{T_r} = \sqrt{C_{T_x}^2 + C_{T_y}^2}$$

Ideal thrust, mv_i, was calculated from the actual mass flow and the dimensionless ideal thrust function based on nozzle pressure ratio. The dimensionless ideal thrust function, $m_i v_i / P_t A^*$, is a function of only the nozzle overall pressure ratio, λ (for a given γ).

$$m_8\, v_{i8} = (A^*/A)_8\, C_{D8} A_8 P_{t8}\, (m_i v_i/P_t A^*)_8$$

where

$$(m_i v_i / P_t A^*) = \gamma \left[\frac{2}{\gamma+1}\right]^{\frac{\gamma}{\gamma-1}} \sqrt{\frac{\gamma+1}{\gamma-1}} \sqrt{1-\lambda^{\frac{1-\gamma}{\gamma}}}$$

$$= 1.81162 \sqrt{1-\lambda^{-0.28571}} \quad \text{for } \gamma = 1.4$$

4.7 Pressure and Temperature Data

Pressure instrumentation for facility and charging station pressures were described previously. Pressures were measured using an Esterline Pressure Systems Inc. (PSI) Netscanner 98RK with Model 9816 multi-ported transducers. All charging station and model pressures were measured with 30 psid range pressure modules. Temperature measurements were obtained using chromel/alumel thermocouples. Temperatures were expressed in °F and °R

4.8 Force Balance Calibration

The force balance calibration determined the output characteristics of the three force balance flexures. Known loads were applied in the axial and vertical directions to obtain a matrix of balance equations, including force interactions, of the form:

$$V_1 = K_{11}B_1 + K_{12}B_2 + K_{13}B_3$$

$$H_o = K_{21}B_1 + K_{22}B_2 + K_{23}B_3$$

$$V_3 = K_{31}B_1 + K_{32}B_2 + K_{33}B_3$$

In the above equations, B_j is the balance output in millivolts for the axial and vertical bridges. K_{ij} terms are the calibration coefficients obtained during the calibration process, where the off-diagonal terms ($i \neq j$) are the interaction correction terms, which numerically have the effect of canceling any interactive load along one axis of the system due to an applied load along an orthogonal axis. The reference coordinate system is defined along the facility centerline and all forces and moments are defined with respect to this coordinate system.

5.0 PRESENTATION OF RESULTS

5.1 ASME Checkout Nozzle Tests

A standard 2.25-inch diameter ASME long-radius flow nozzle was tested to demonstrate proper facility operation and accuracy in determining C_D and C_T of static test nozzles.

The ASME test results are tabulated in Figure 5 and are plotted in Figures 6a-c with the predicted (or target) value curves. The target-value curves are based on semi-empirical equations consistent with those described for the ASME meter in Sections 4.3 and 4.5. Photographs of the ASME nozzle are shown in Figure 4.

The test results were statistically analyzed for bias (average difference between actual and predicted values) and scatter (standard deviation of the individual biases from the overall bias). This analysis is summarized in the following table.

Static Checkout Results with ASME Nozzles

			Average Bias		Standard Deviation (±):	
Test Series	**λ Range**	**N**	**C_T**	**C_D**	**C_T**	**C_D**
2.25” ASME Pretest	**1.6 – 3.0**	**16**	**-0.0001**	**0.0006**	**0.0004**	**0.0005**
	1.2 - 1.6	6	-0.0003	-0.0006	0.0016	0.0011
2.25” ASME Post Test	**1.6 - 2.4**	**10**	**0.0001**	**0.0008**	**0.0007**	**0.0006**
	1.1 - 1.4	6	0.0026	-0.0004	0.0012	0.0008

5.2 Model Tests

The model configuration definitions are provided in Figure 8. Photographs of the test configurations are contained in Figures 9a-i. Model test conditions and major test results for the static tests are tabulated in Figure 10. The tabulations include: configuration, data point number, actual values of independent test variables (λ_8, P_{t_8}, T_{t_8}, P_{amb}, T_{amb}), and major test results (W_8, C_{T_r}, C_{D_8}, α, and L_y). Results are plotted in Figures 11 through 13. Nozzle thrust coefficients are plotted in Figures 11a-b. Nozzle discharge coefficients are plotted in Figures 12a-b. Thrust vector angles are plotted in Figure 13.

Detailed data, model assembly inspections, and calculations are contained in a separate Data Appendix. A DVD-ROM containing all model data and accompanying information is also included with the Appendix. Data and photos were also transmitted to NASA via email as testing progressed.

6.0 REFERENCES

1 Wyatt, DeMarquis D., "Analysis of Errors Introduced by Several Methods of Weighting Non-Uniform Duct Flows." NACA TN 3400. March 1955.

2. Jordan, D.P., and Mintz, M.D., "Air Tables." McGraw-Hill Book Company, New York. 1965.

3 Reimer, R.M., "Computation of the Critical Flow Function, Pressure Ratio, and Temperature Ratio for Real Air." ASME Paper #62-WA-177.1962.

4. Ames Research Staff, "Equations, Tables, and Charts for Compressible Flow." NACA Report 1135. 1953.

5. Johnson, R.C., "Real-Gas Effects in Critical-Flow-Through Nozzles and Tabulated Thermodynamic Properties." NASA TN D-2565. 1965.

6. Mikkelsen, K.L., and Brasket, R.G., "An Equation Set for ASME Nozzle Discharge and Thrust Coefficients." AIAA 2011-1265. 2011.

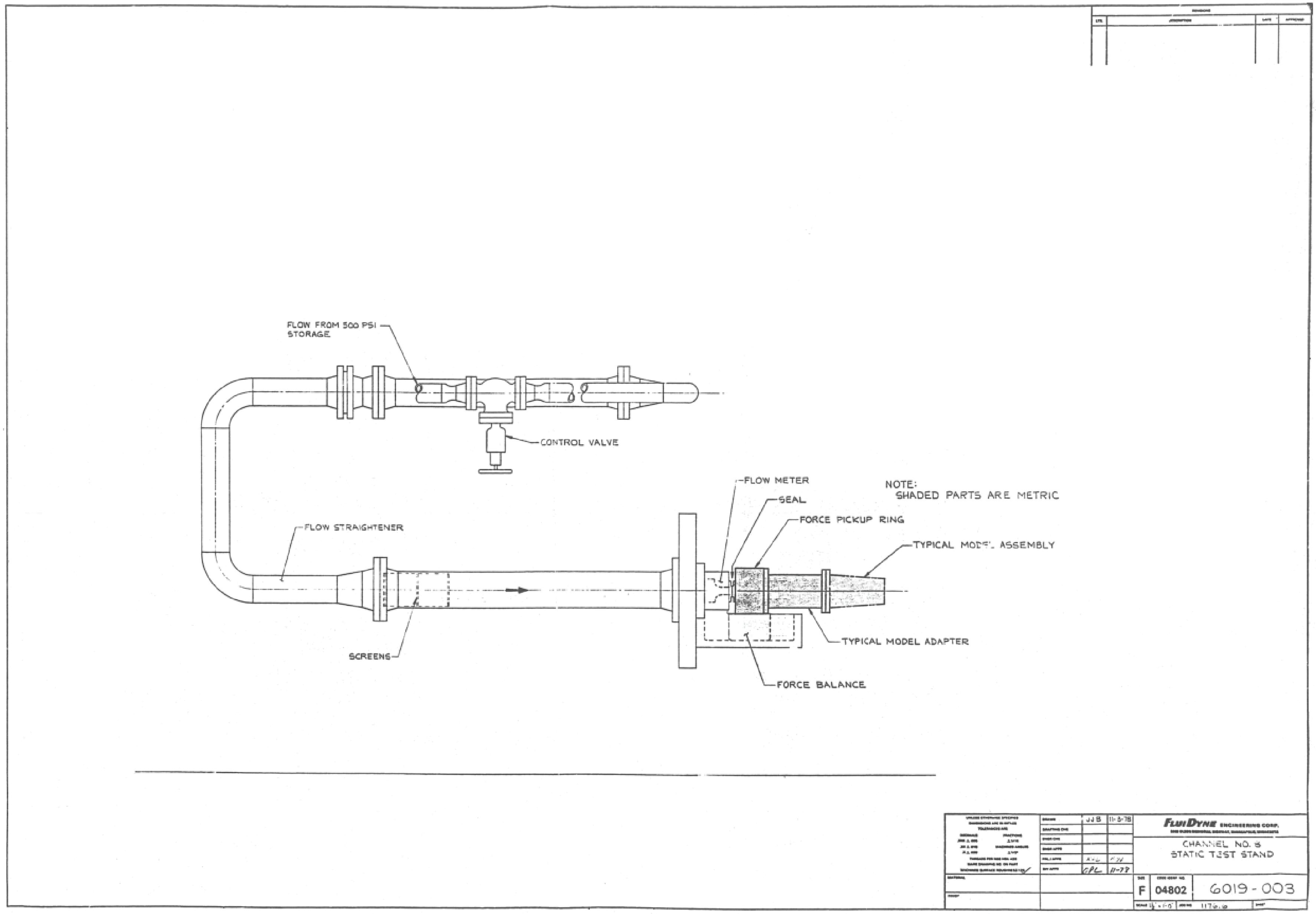

FIGURE 1. CHANNEL 8 STATIC THRUST STAND

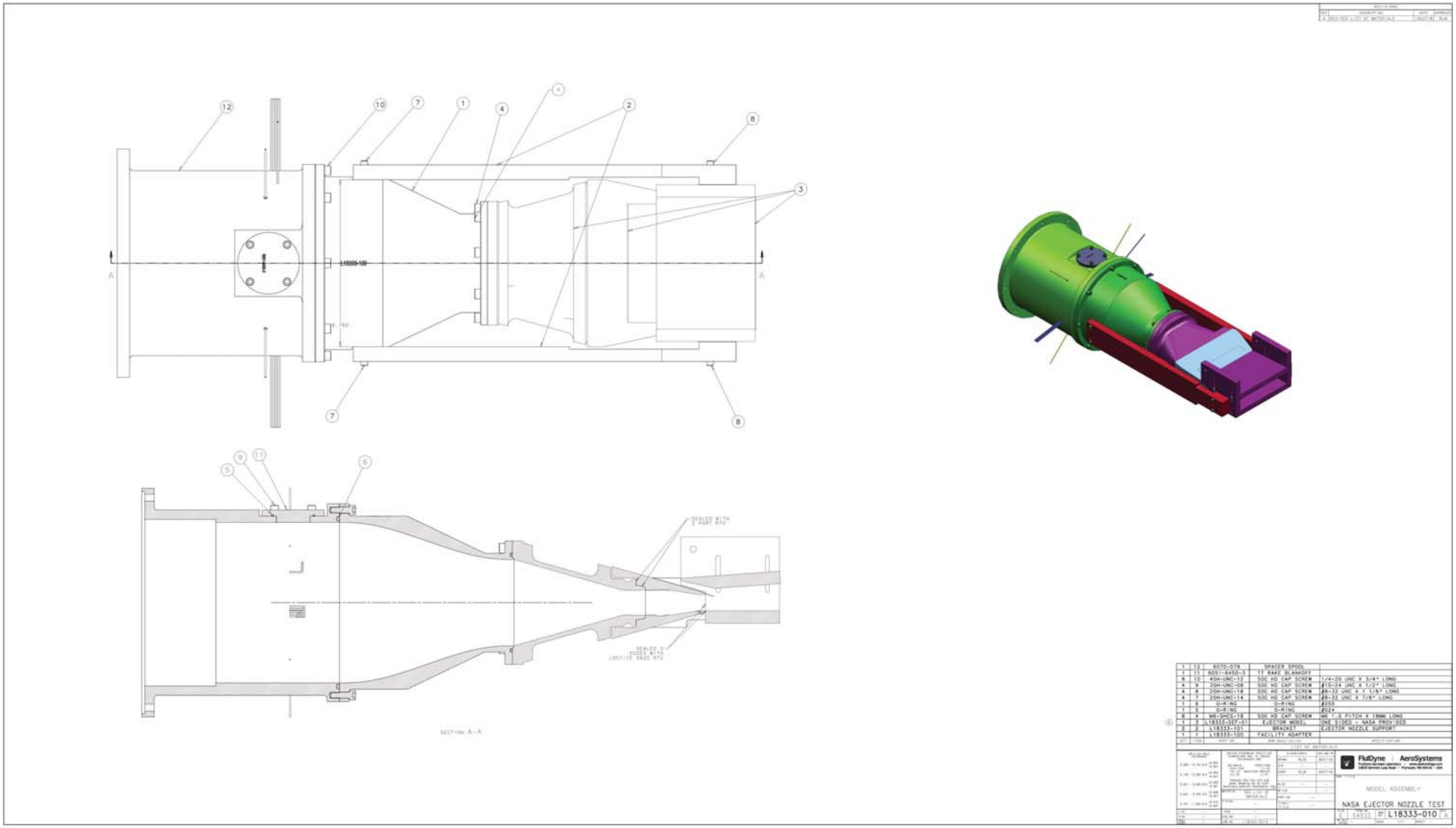

**FIGURE 2. MODEL ASSEMBLY
NASA EJECTOR NOZZLE TEST
(DRAWING L18333-010)**

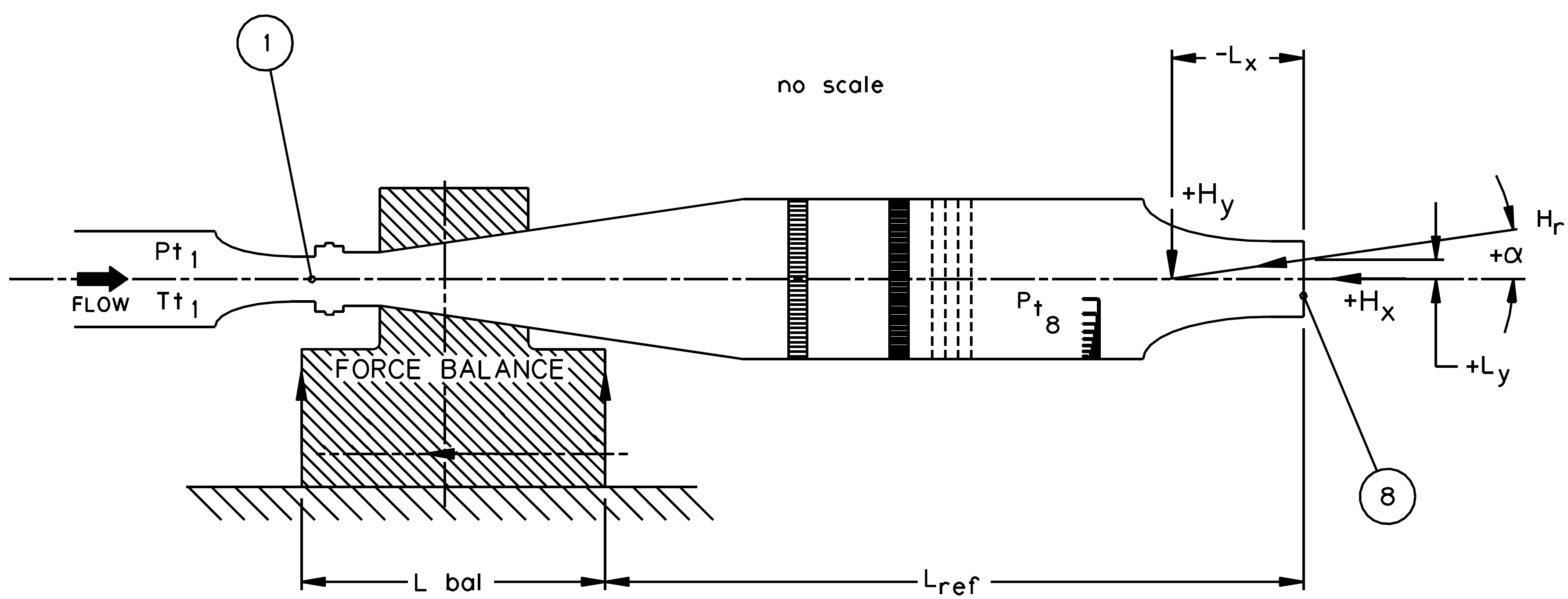

Station	Description
1	Flow meter throat
8	Nozzle throat

FIGURE 3. STATION NOTATION, ASME CHECKOUT NOZZLE TESTS

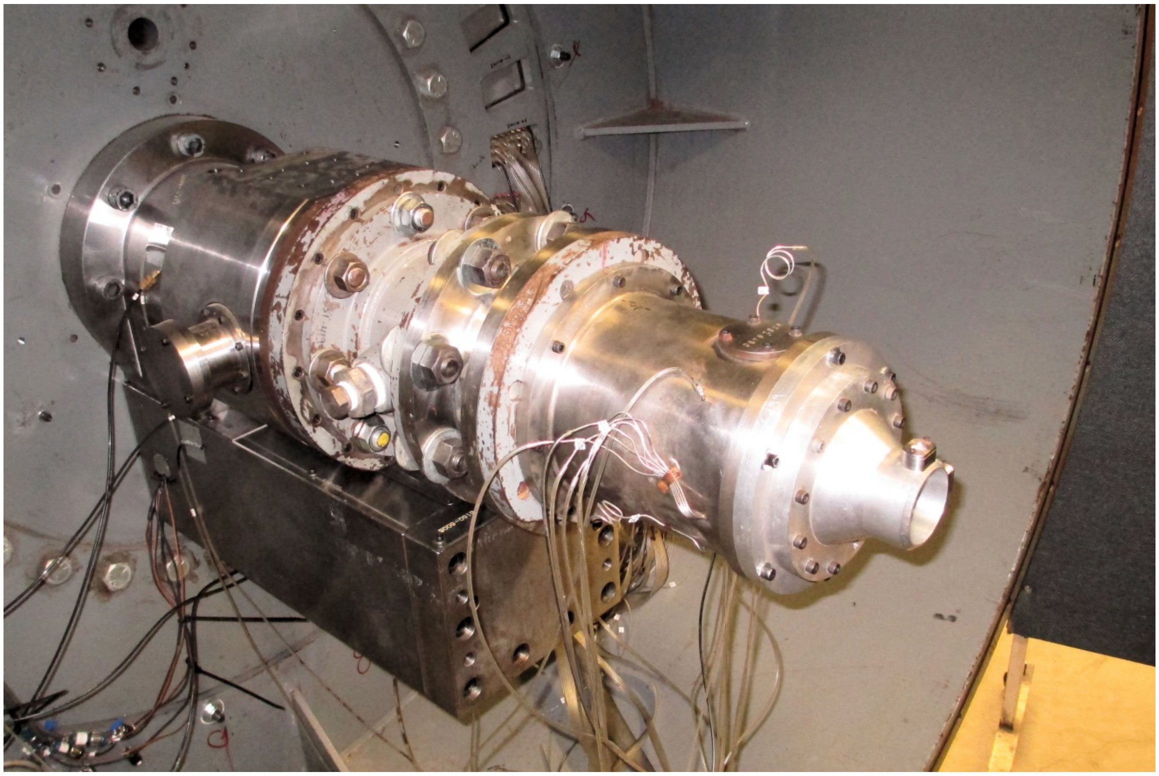

Duct assembly and charging station with 2.25-inch ASME nozzle.

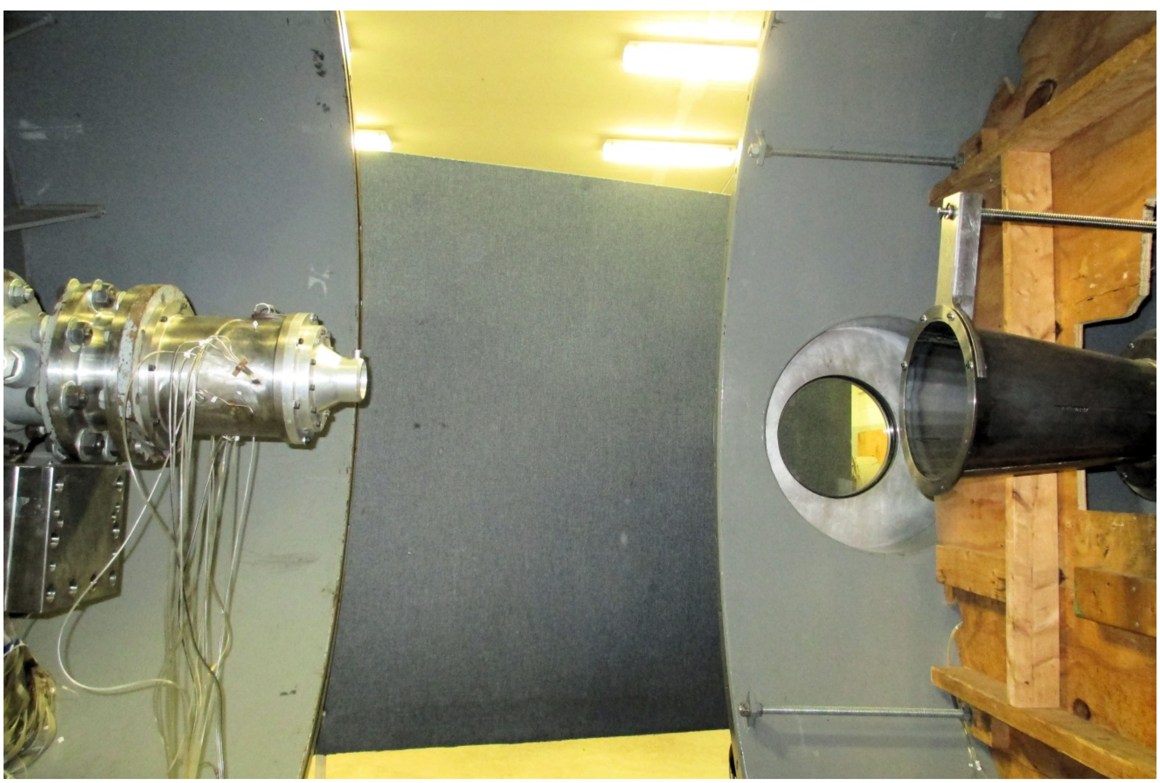

2.25” ASME nozzle assembly, conical collector and 6 inch diffuser.
(Test cabin was in the open position for all tests.)

FIGURE 4. ASME CHECKOUT NOZZLE PHOTOGRAPHS

L18333, Channel 8

Data Point	λ	P_t	P_a	C_{Tr}	C_D	α (degrees)	L_y (in.)
Pretest to Atmosphere							
601.01	2.994	42.424	14.170	0.9904	0.9913	0.16	-0.01
601.02	2.992	42.387	14.165	0.9907	0.9914	0.16	-0.01
602.02	2.795	39.581	14.164	0.9924	0.9916	0.13	-0.03
602.03	2.796	39.595	14.162	0.9925	0.9916	0.14	-0.03
603.02	2.591	36.745	14.182	0.9941	0.9907	0.15	-0.03
603.03	2.591	36.738	14.178	0.9942	0.9907	0.15	-0.04
604.02	2.395	33.958	14.182	0.9950	0.9909	0.12	-0.05
604.03	2.394	33.932	14.177	0.9948	0.9911	0.12	-0.05
605.02	2.193	31.057	14.164	0.9946	0.9910	0.08	-0.08
605.03	2.196	31.098	14.162	0.9950	0.9912	0.09	-0.08
606.01	1.990	28.248	14.197	0.9947	0.9909	0.09	-0.08
606.03	1.994	28.272	14.177	0.9947	0.9907	0.07	-0.09
607.01	1.791	25.425	14.197	0.9936	0.9909	0.12	-0.08
607.02	1.794	25.447	14.182	0.9933	0.9907	0.08	-0.10
608.01	1.585	22.459	14.170	0.9932	0.9915	0.04	-0.14
608.02	1.586	22.467	14.162	0.9932	0.9915	0.03	-0.15
609.02	1.393	19.749	14.182	0.9929	0.9917	0.07	-0.14
609.03	1.394	19.760	14.177	0.9936	0.9917	0.03	-0.17
610.01	1.195	16.963	14.198	0.9890	0.9892	0.22	-0.13
610.03	1.195	16.939	14.177	0.9888	0.9891	0.08	-0.19

2.25 inch nozzle (6051-6245)

FIGURE 5. TABULATION OF ASME CHECKOUT NOZZLE TEST RESULTS (SHEET 1 OF 2)

L18333, Channel 8

Data Point	λ	P_t	P_a	C_{Tr}	C_D	α (degrees)	L_y (in.)
Posttest to Atmosphere							
611.01	2.992	42.496	14.201	0.9903	0.9918	0.20	0.04
611.02	2.992	42.489	14.203	0.9907	0.9917	0.22	0.04
612.01	2.793	39.661	14.202	0.9923	0.9916	0.20	0.03
612.02	2.793	39.672	14.203	0.9926	0.9917	0.19	0.02
613.01	2.593	36.847	14.210	0.9940	0.9912	0.20	0.02
613.02	2.587	36.772	14.212	0.9941	0.9916	0.19	0.01
614.01	2.399	34.090	14.210	0.9951	0.9910	0.18	0.00
614.02	2.400	34.110	14.211	0.9951	0.9915	0.16	-0.01
615.03	2.195	31.187	14.210	0.9953	0.9909	0.15	-0.02
615.06	2.195	31.540	14.367	0.9953	0.9911	0.17	-0.01
616.03	1.999	28.403	14.210	0.9951	0.9909	0.14	-0.03
616.05	1.995	28.664	14.366	0.9946	0.9907	0.16	-0.02
617.03	1.800	25.577	14.210	0.9943	0.9909	0.15	-0.05
617.06	1.790	25.718	14.367	0.9942	0.9912	0.17	-0.04
618.01	1.588	22.560	14.210	0.9944	0.9914	0.14	-0.08
618.04	1.593	22.880	14.366	0.9938	0.9915	0.15	-0.07
619.01	1.394	19.808	14.210	0.9945	0.9918	0.13	-0.11
619.04	1.394	20.035	14.377	0.9951	0.9916	0.18	-0.09
620.04	1.198	17.220	14.377	0.9950	0.9895	0.21	-0.14
620.05	1.196	17.195	14.381	0.9952	0.9899	0.20	-0.15

2.25 inch nozzle (6051-6245)

FIGURE 5. TABULATION OF ASME CHECKOUT NOZZLE TEST RESULTS (SHEET 2 OF 2)

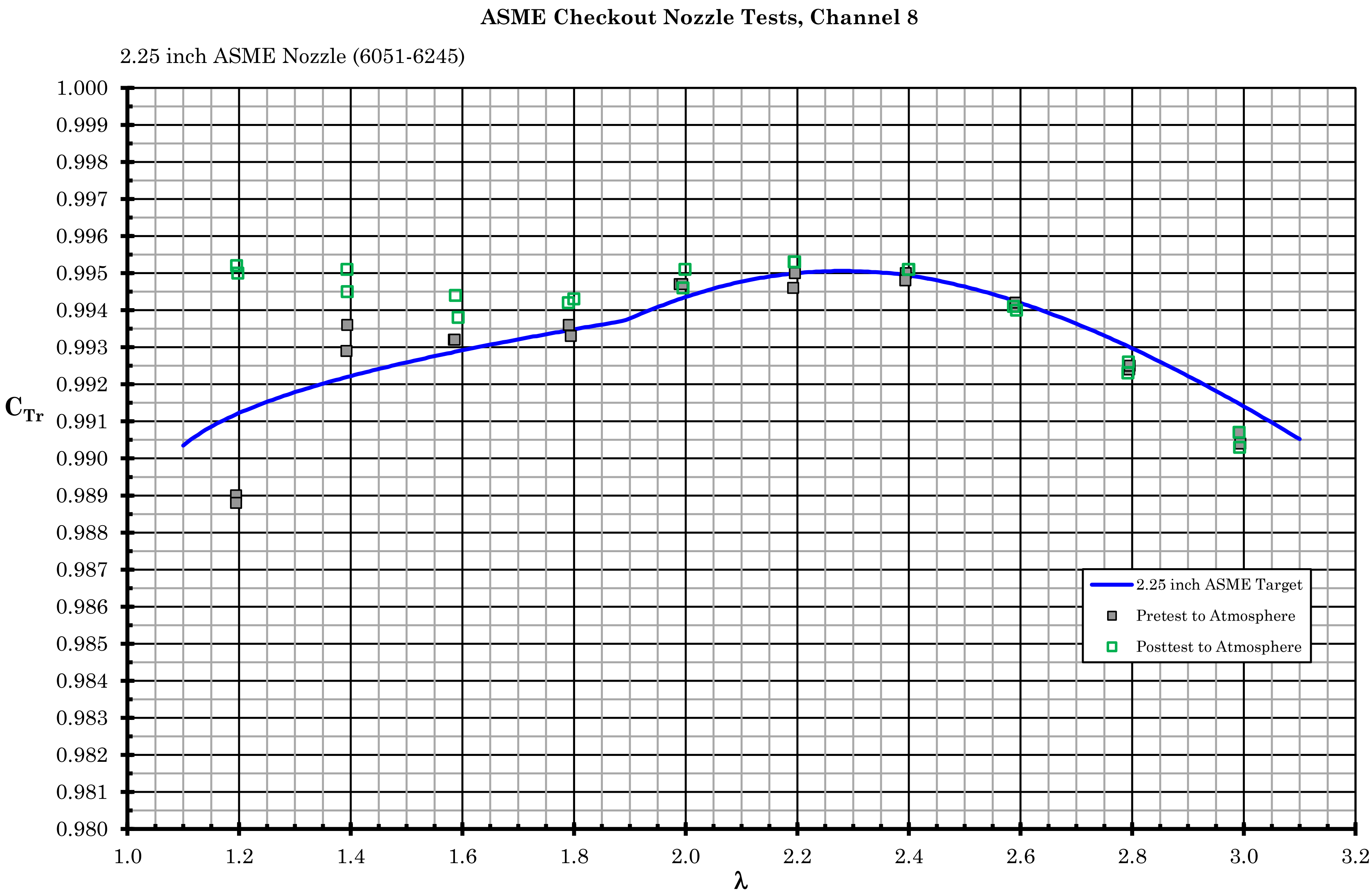

FIGURE 6a. THRUST COEFFICIENTS, 2.25 INCH ASME NOZZLE

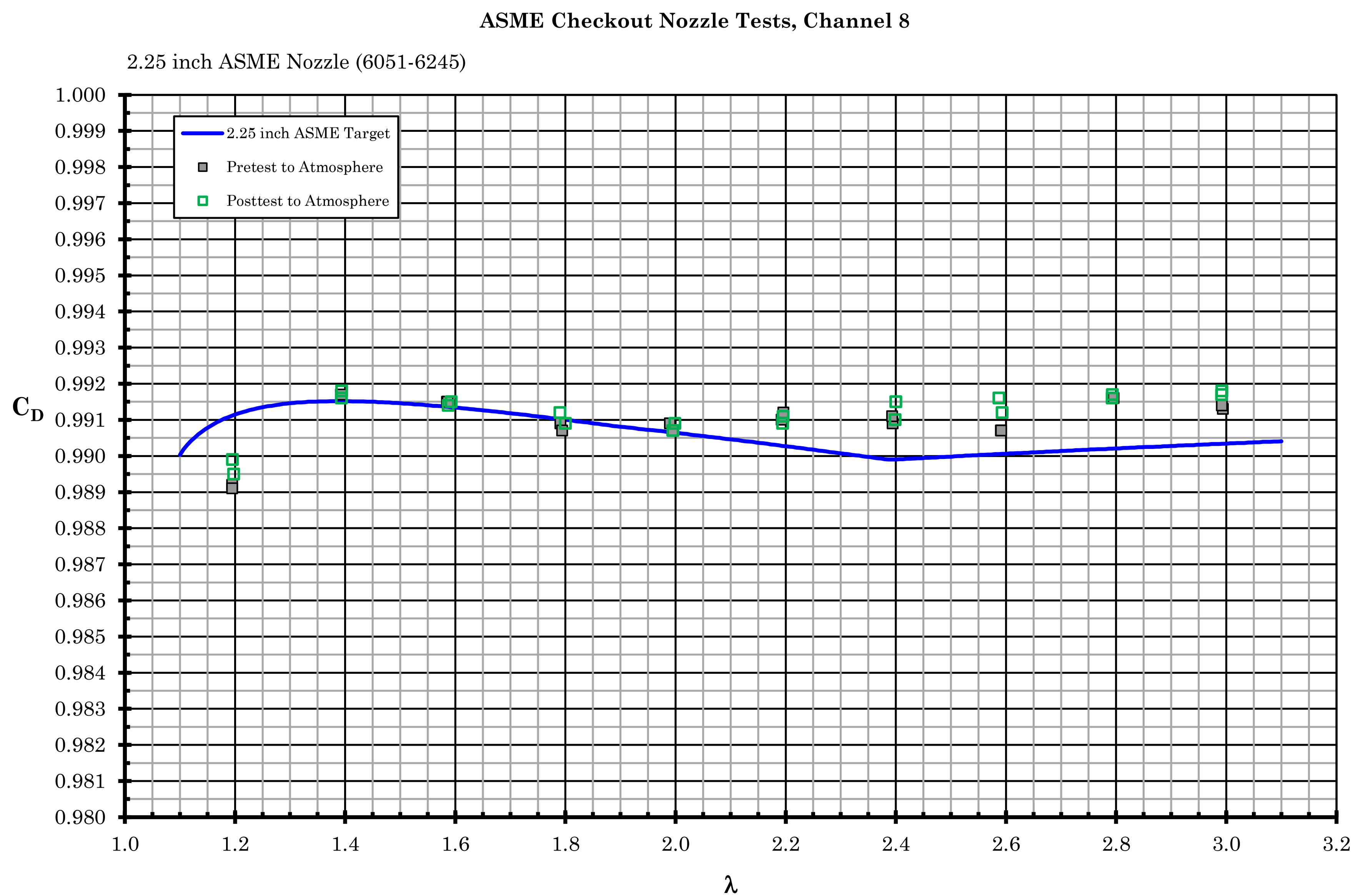

FIGURE 6b. DISCHARGE COEFFICIENTS, 2.25 INCH ASME NOZZLE

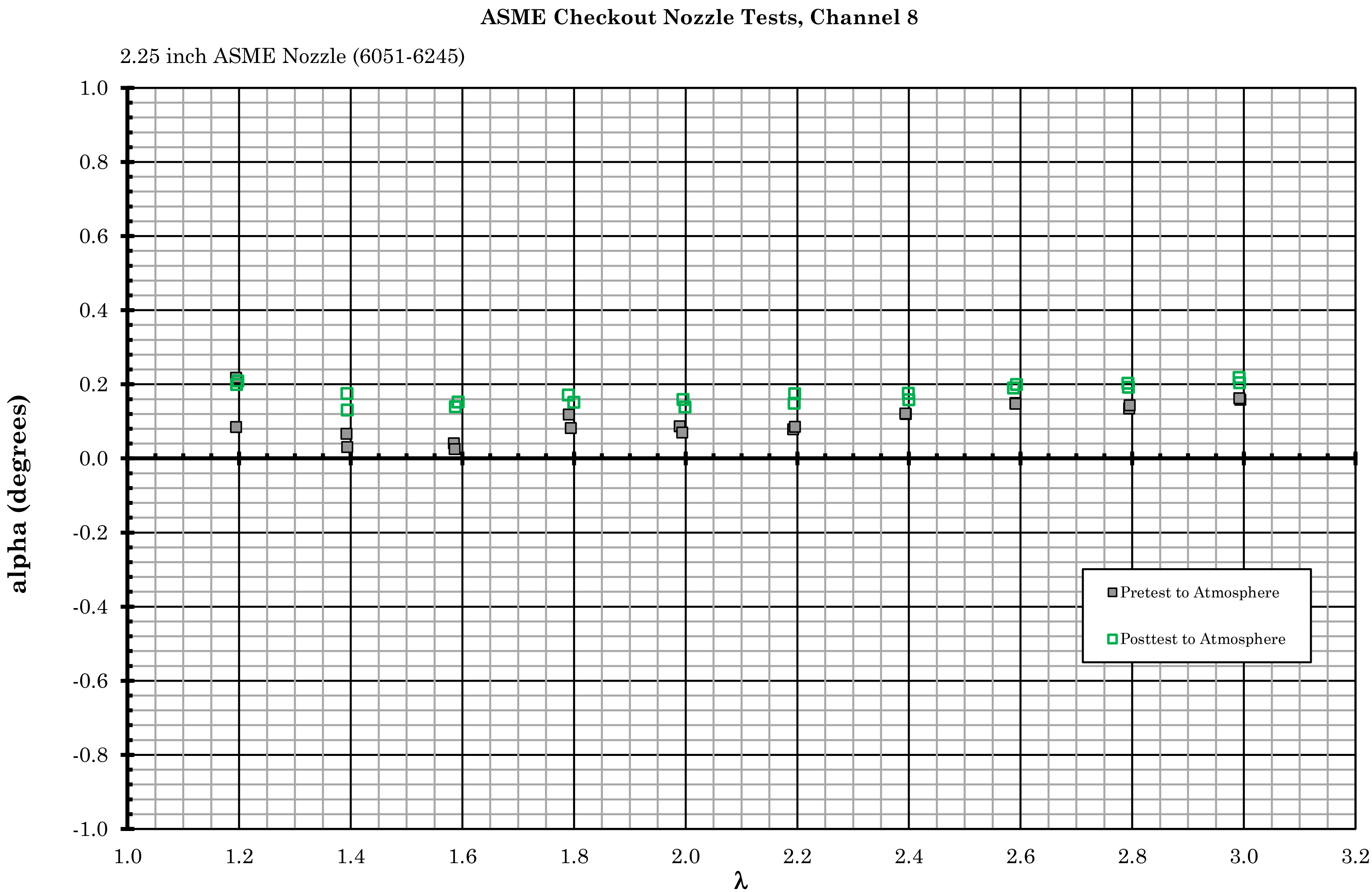

FIGURE 6c. THRUST VECTOR ANGLES, 2.25 INCH ASME NOZZLE

(no scale)

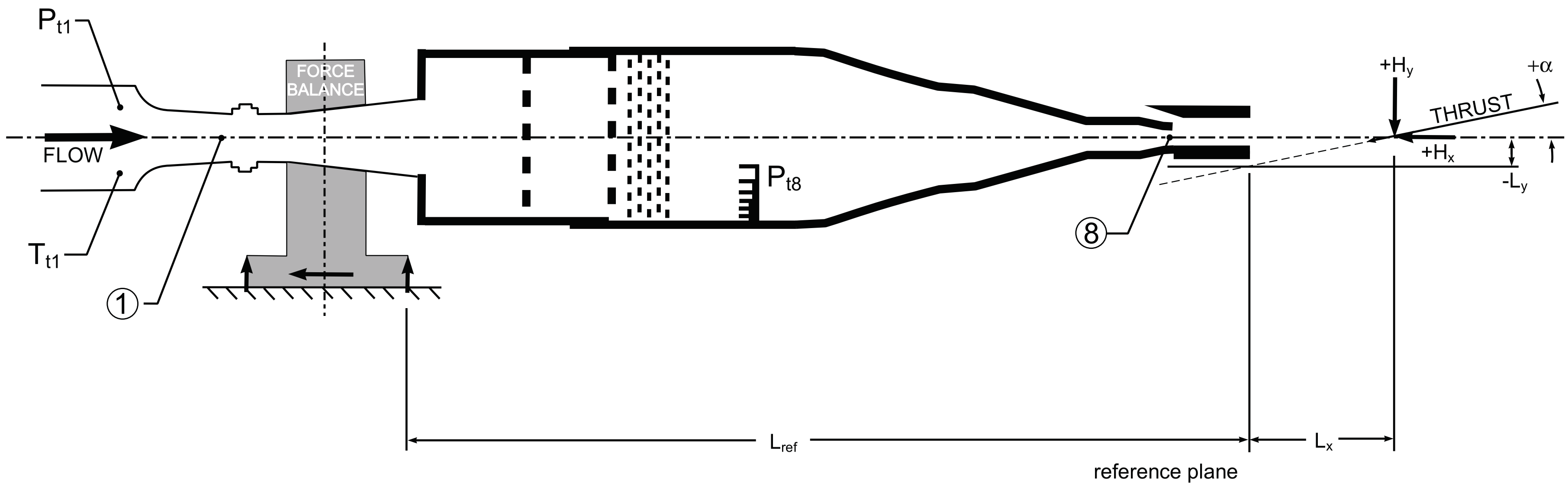

Station	Description
1	ASME meter throat
8	Core nozzle

FIGURE 7. STATION NOTATION, MODEL TESTS

L18333 NASA One-Sided Ejector Nozzle - Model Test Configuration Definition

Config. Number	Description	Data Point Numbers	Tab Strip *	Target Values for: G (in.)	H (in.)	Inspected Values for: Average G (in.)	Average H (in.)	Upstream Plugs	Downstream Plugs
1	Baseline with no tab strip	1 - 6	no	0.249	0.900	0.264	0.903	32H	32H
2	Baseline with tab strip installed	7 - 12	yes	0.235	0.900	0.230	0.903	32H	32H
3	Larger slot and exit areas with tab strip	13 - 18	yes	0.380	1.050	0.381	1.055	47H	47H
4	Divergent upper plate with tab strip	19 - 24	yes	0.170	1.080	0.169	1.107	35H	48H

A constant value of $A_8 = 3.54$ in^2 was used in the data reduction for all configurations as specified by NASA.

* NASA part numbers were not specified. The tab strip that was installed had been previously used during NASA acoustic testing.

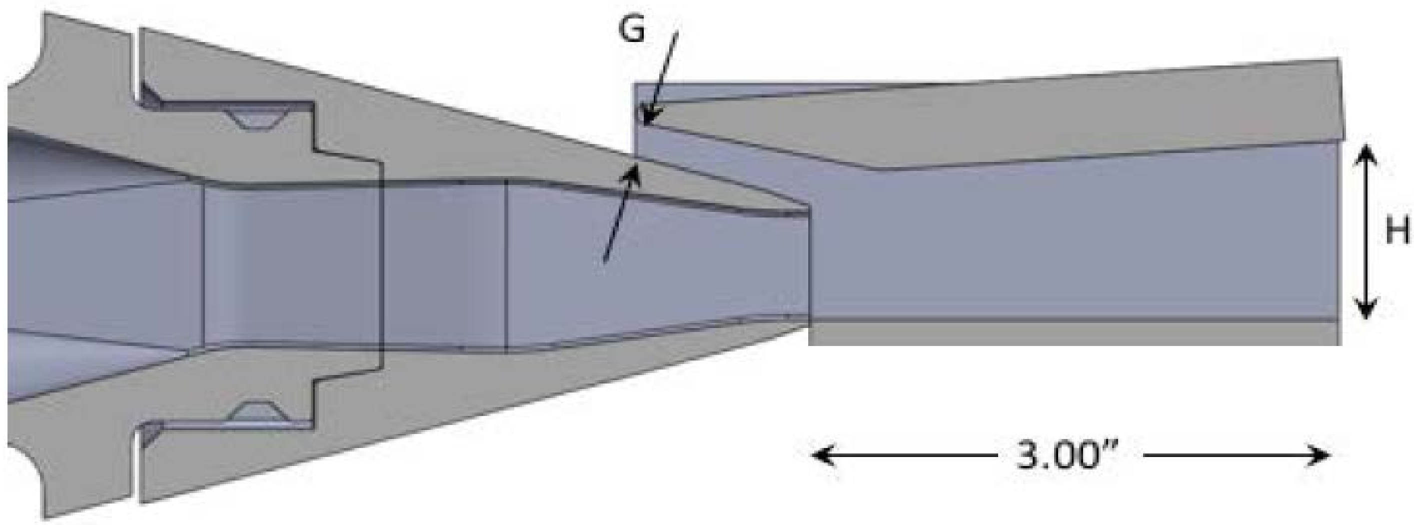

FIGURE 8. MODEL CONFIGURATION DEFINITION

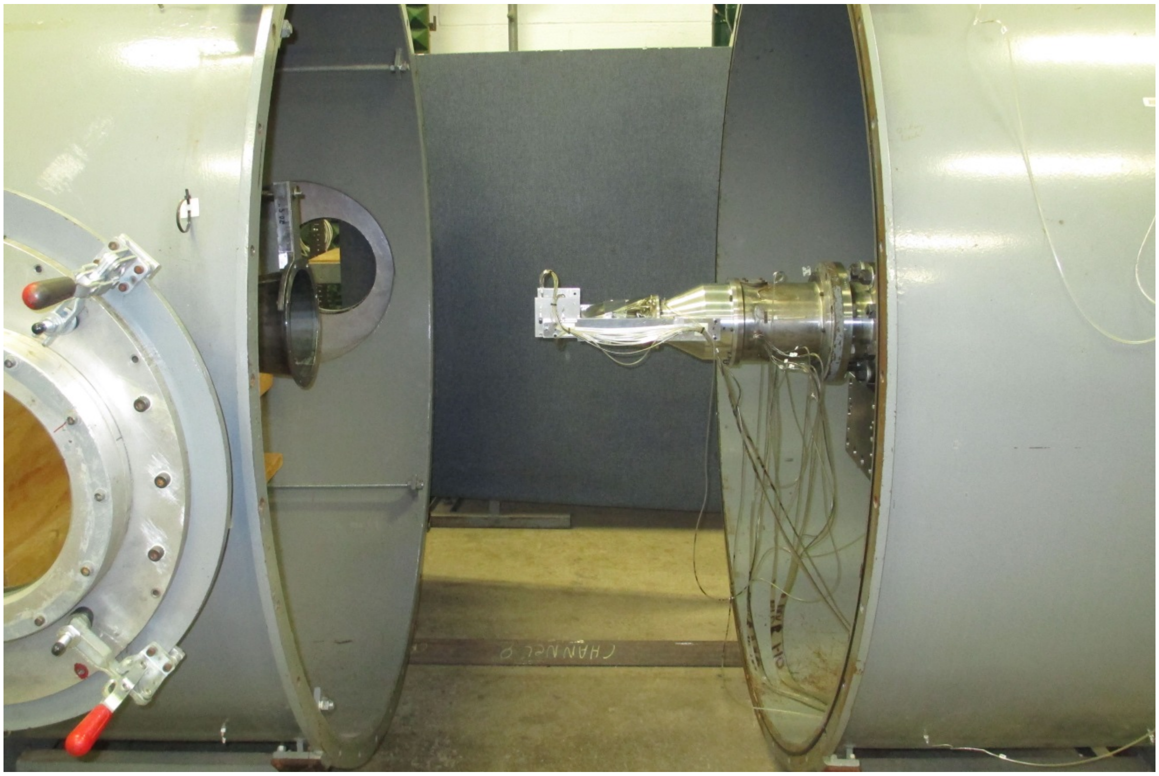

NASA one-sided ejector nozzle model installation in Channel 8 test facility.
(flow is from right to left in these photos)

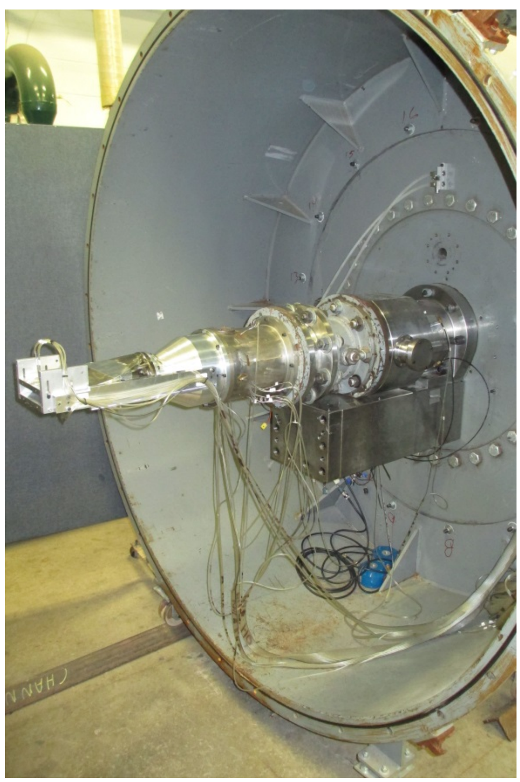

Model and facility adapter installation.

FIGURE 9a. MODEL PHOTOGRAPHS

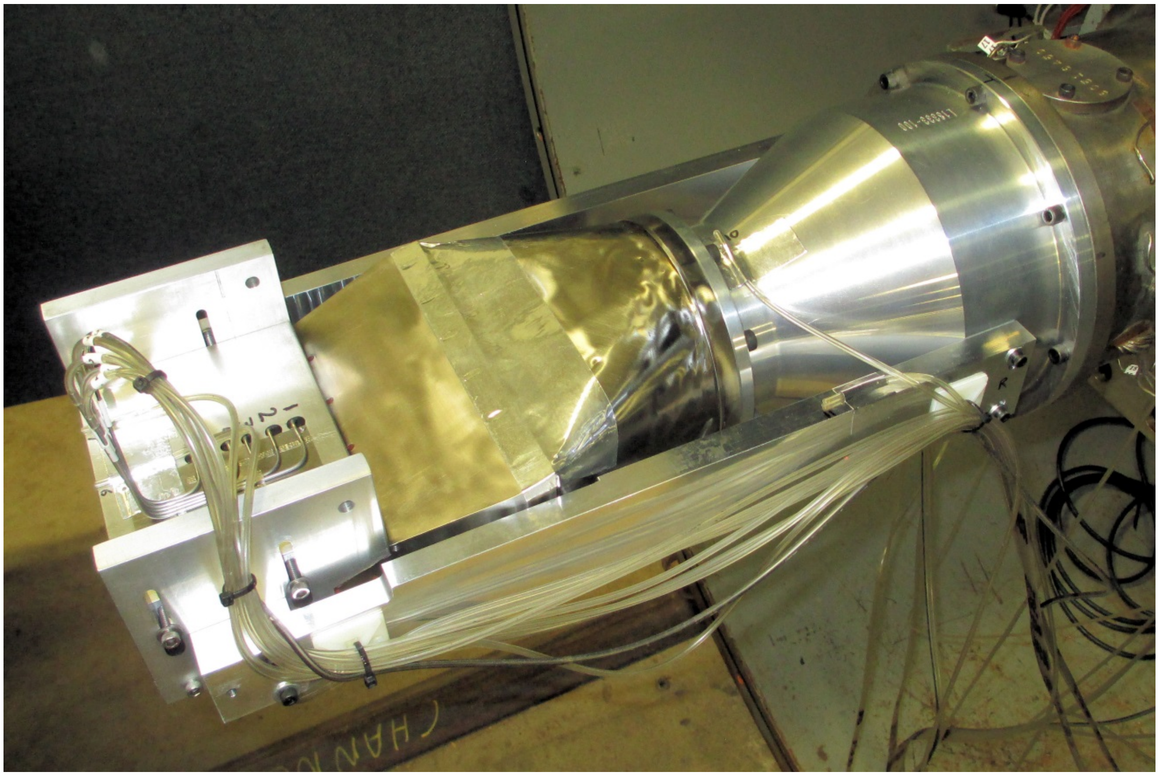

Config 1 - Baseline: NASA one-sided ejector nozzle system.

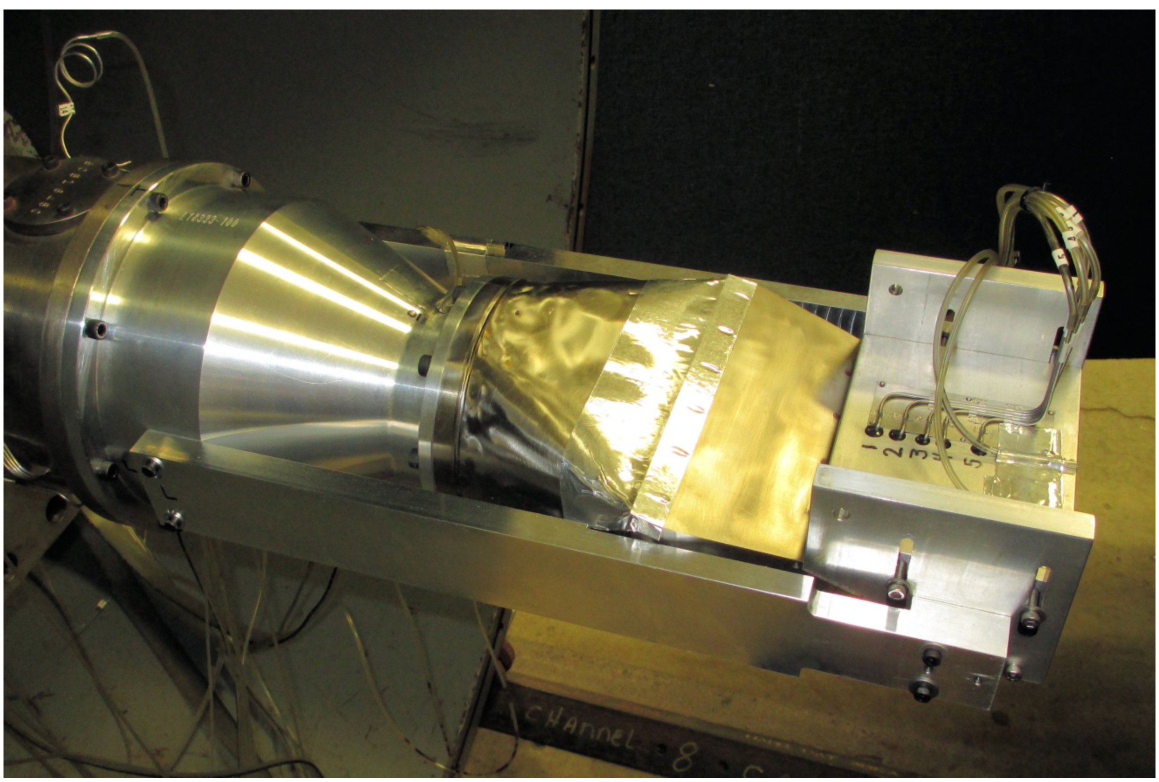

FIGURE 9b. MODEL PHOTOGRAPHS

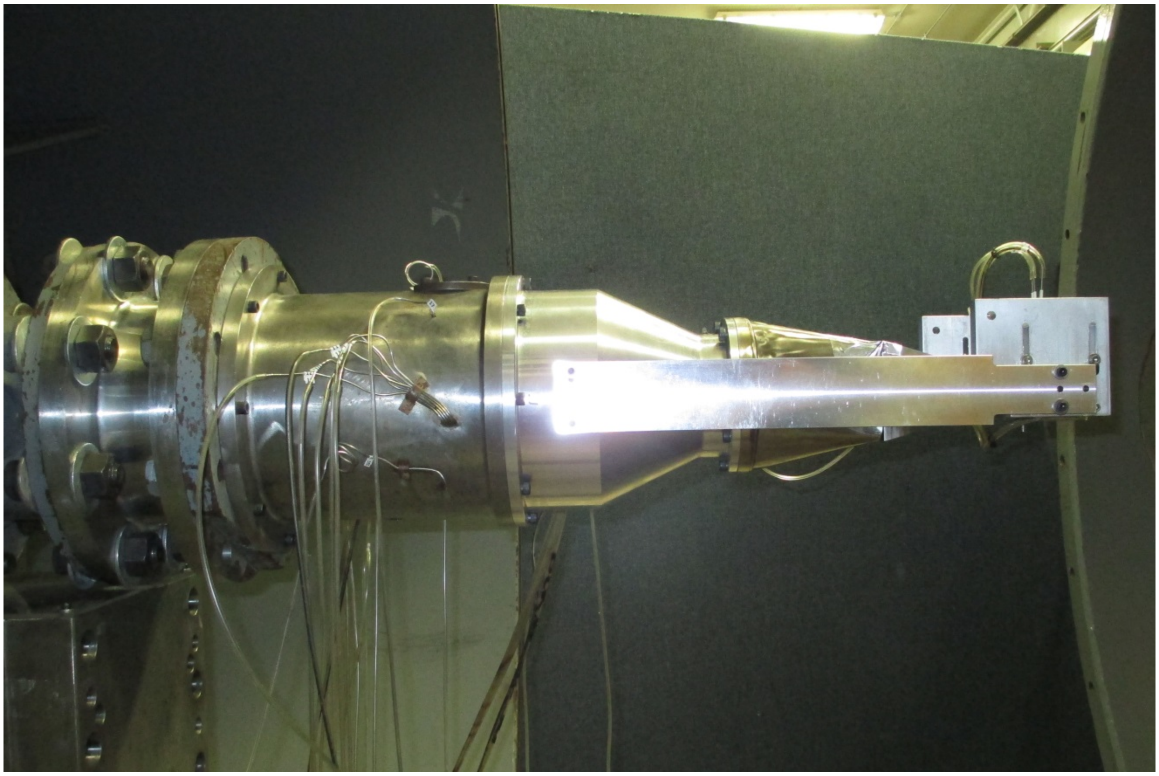

Config 1 - Baseline: side view. (flow is from left to right)

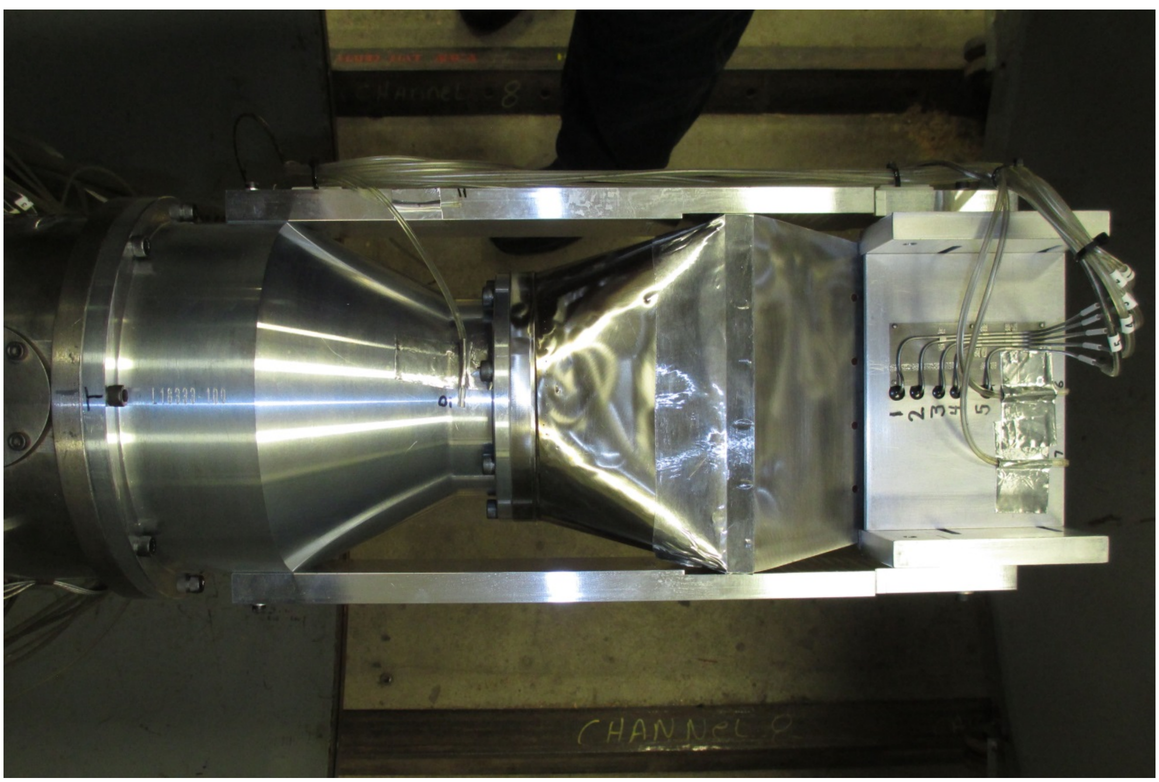

Config 1 - Baseline: top view. (flow is from left to right)

FIGURE 9c. MODEL PHOTOGRAPHS

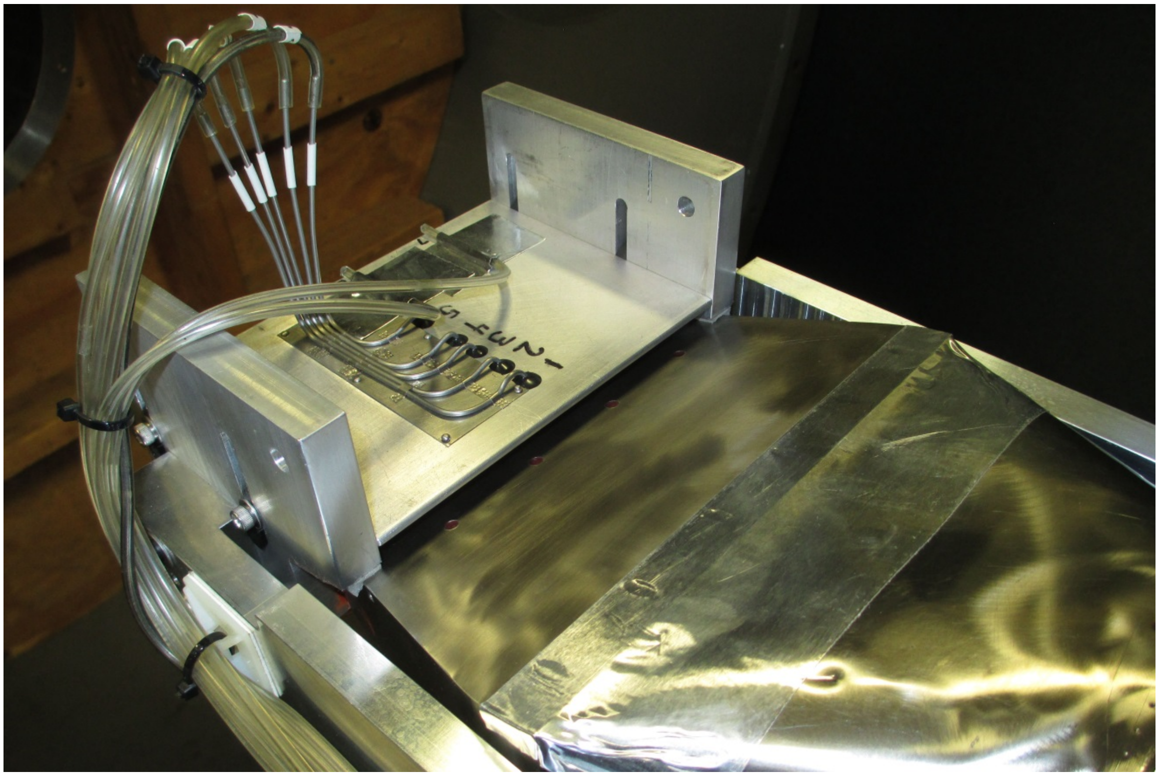

Config 1 - Baseline: view of ejector box flow entry slot.

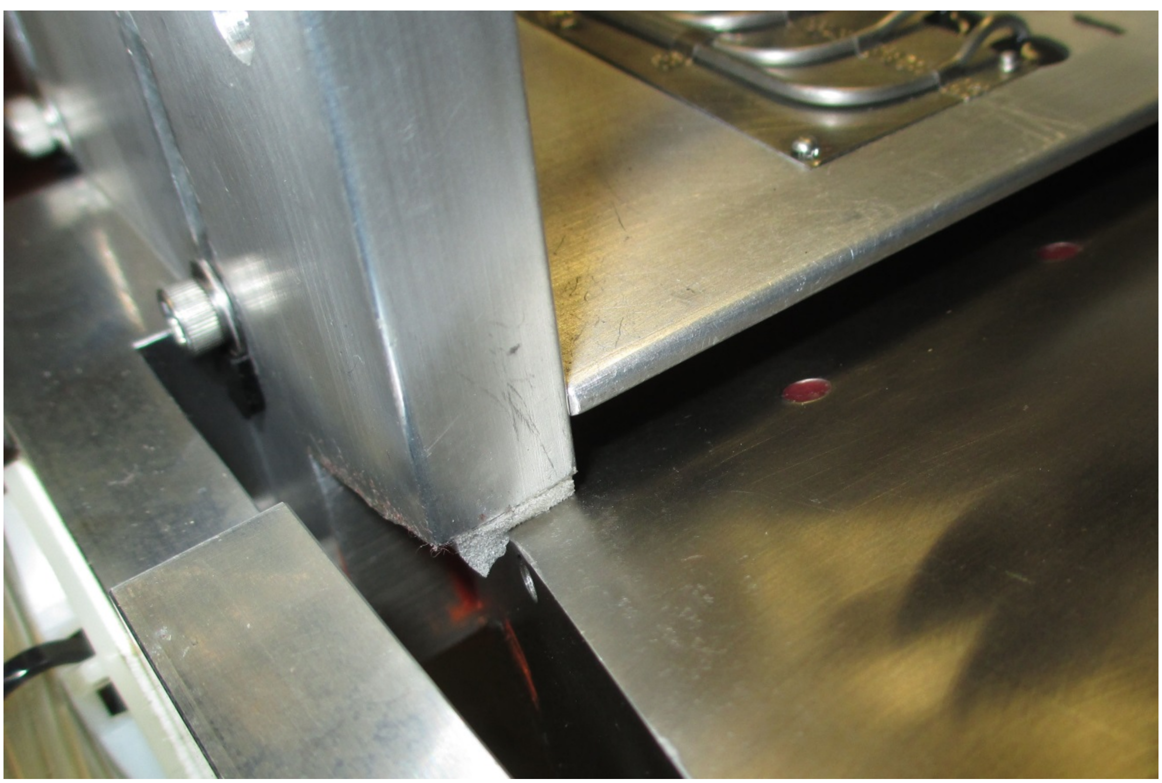

Foam sealing tape used to fill gaps between box side walls and nozzle surface.

FIGURE 9d. MODEL PHOTOGRAPHS

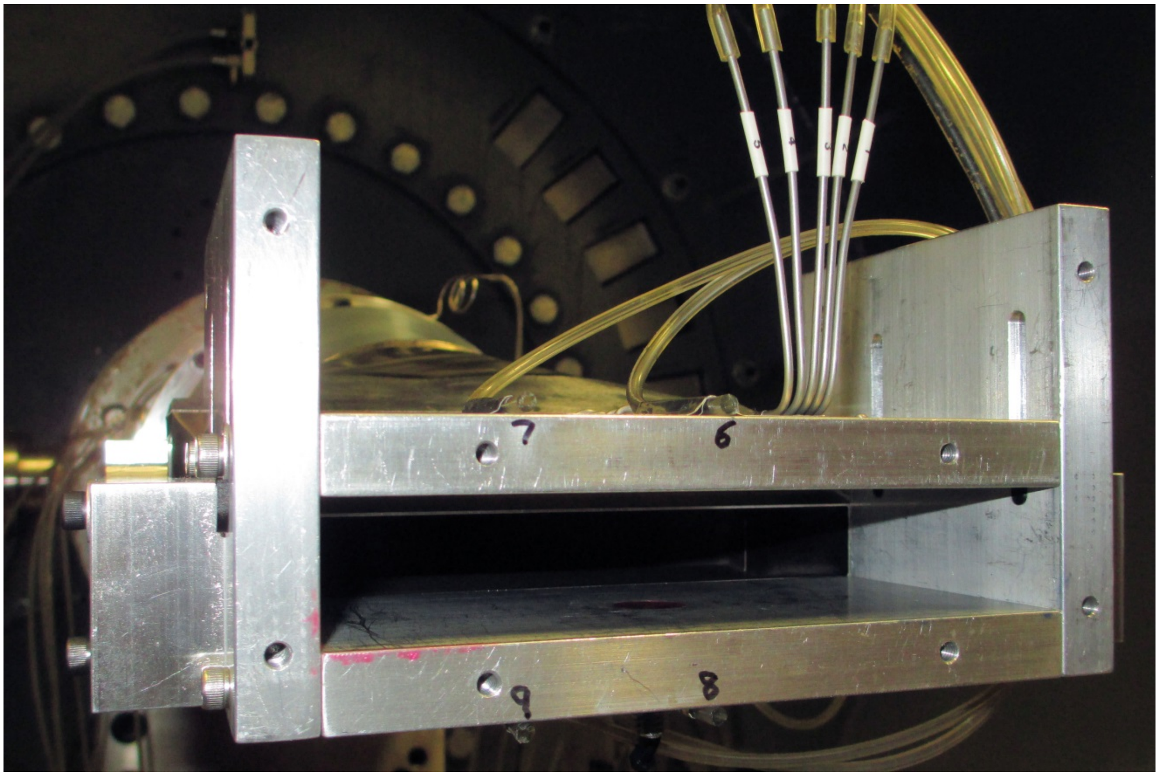

Config 1 - Baseline: exit of ejector box.

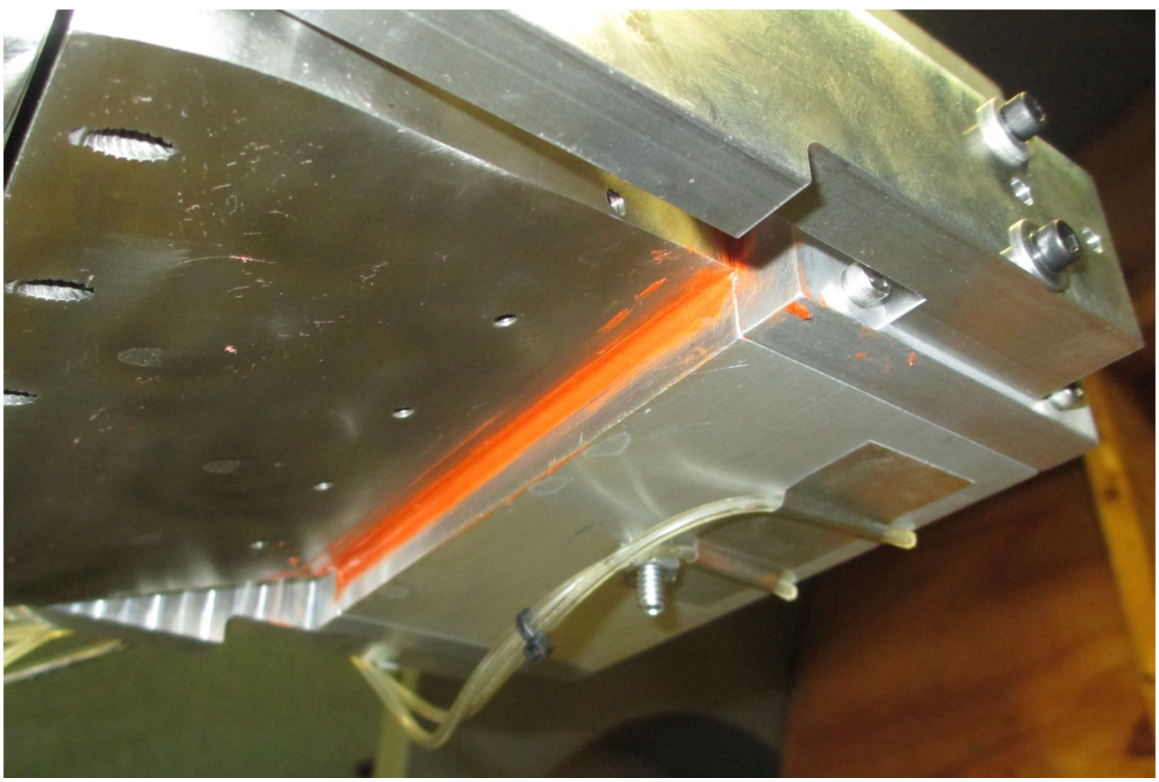

RTV applied externally to joint between nozzle and ejector box.

FIGURE 9e. MODEL PHOTOGRAPHS

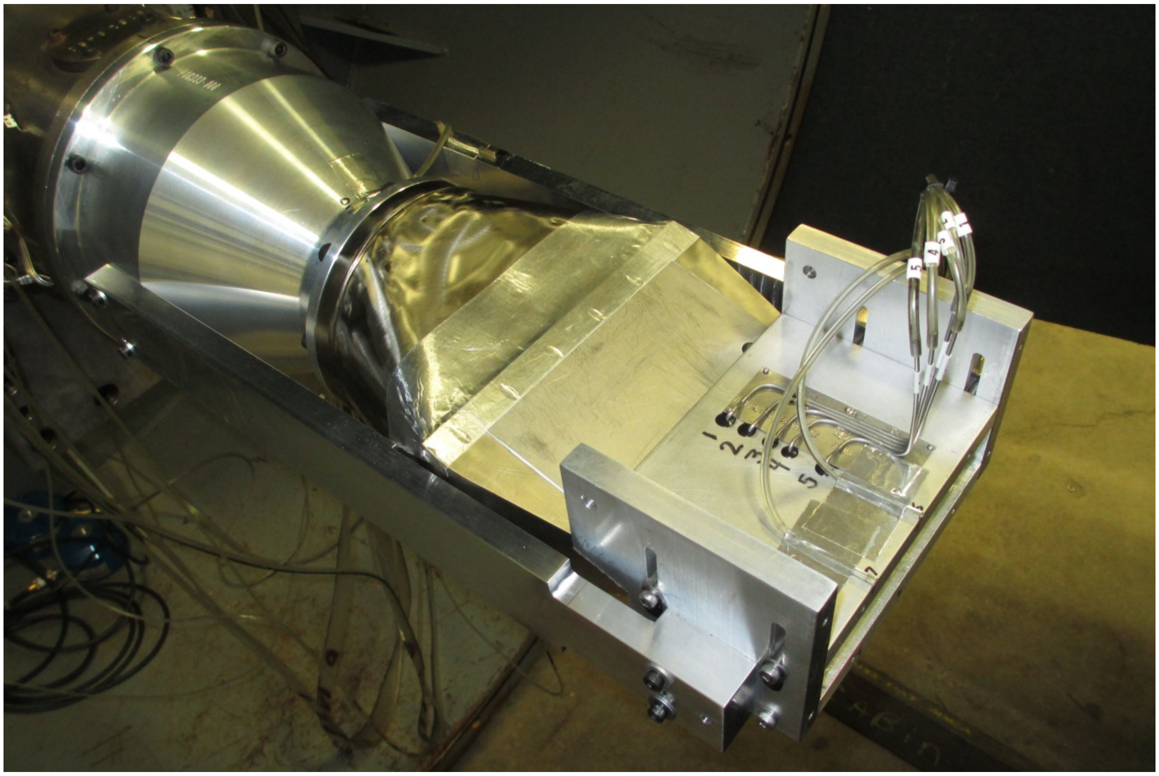

Config 2 – Tab Strip: baseline configuration with addition of serrated tab strip to nozzle.

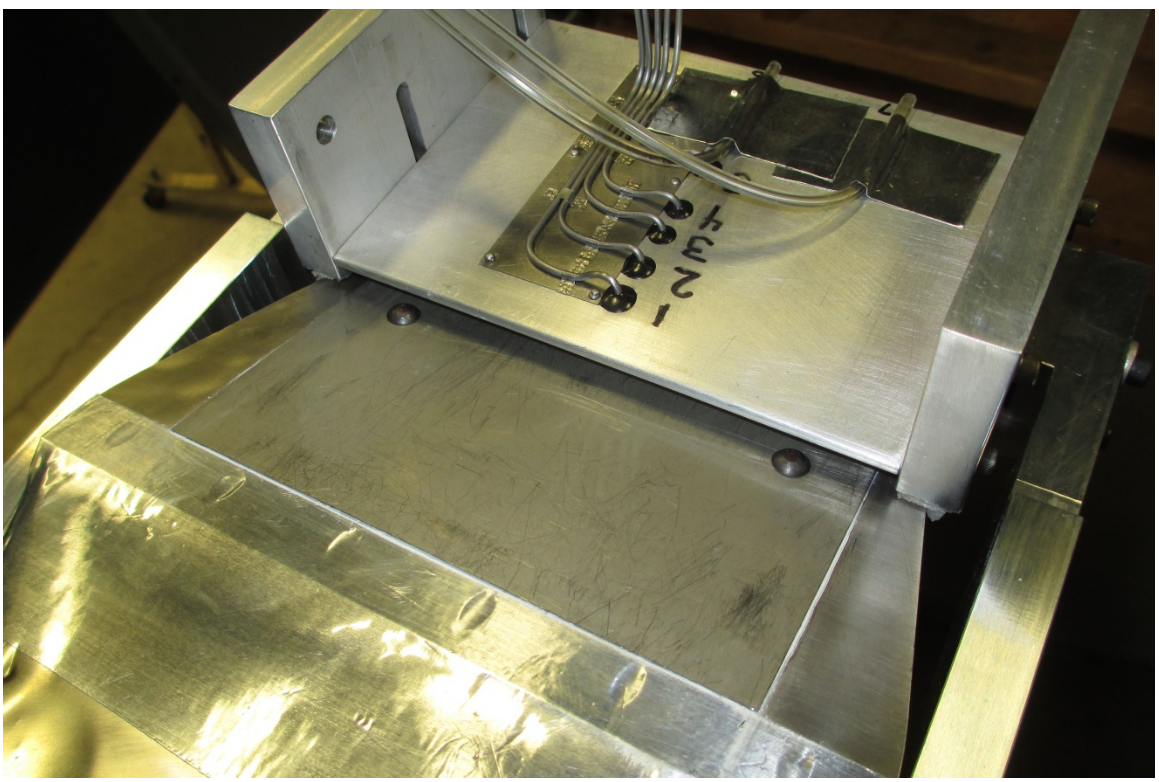

Tab strip attached to nozzle upper surface using epoxy and screws.

FIGURE 9f. MODEL PHOTOGRAPHS

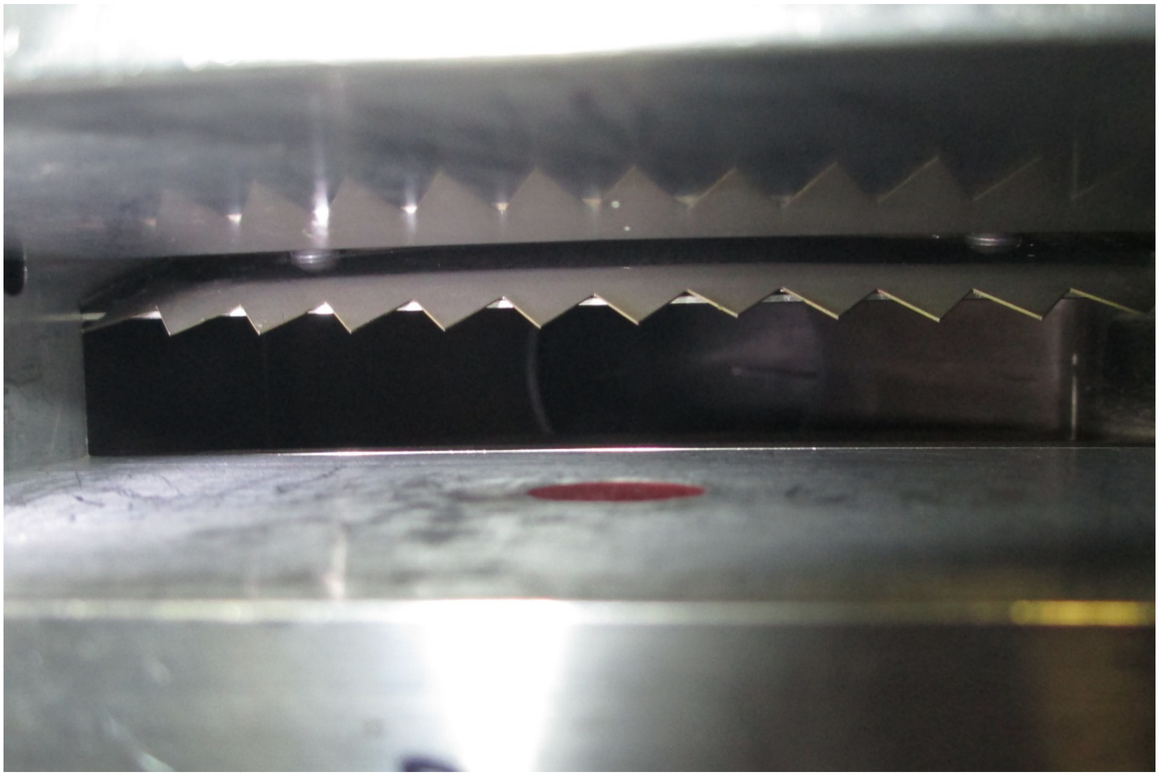

Config 2 – Tab Strip: view inside ejector box of serrated tab strip.

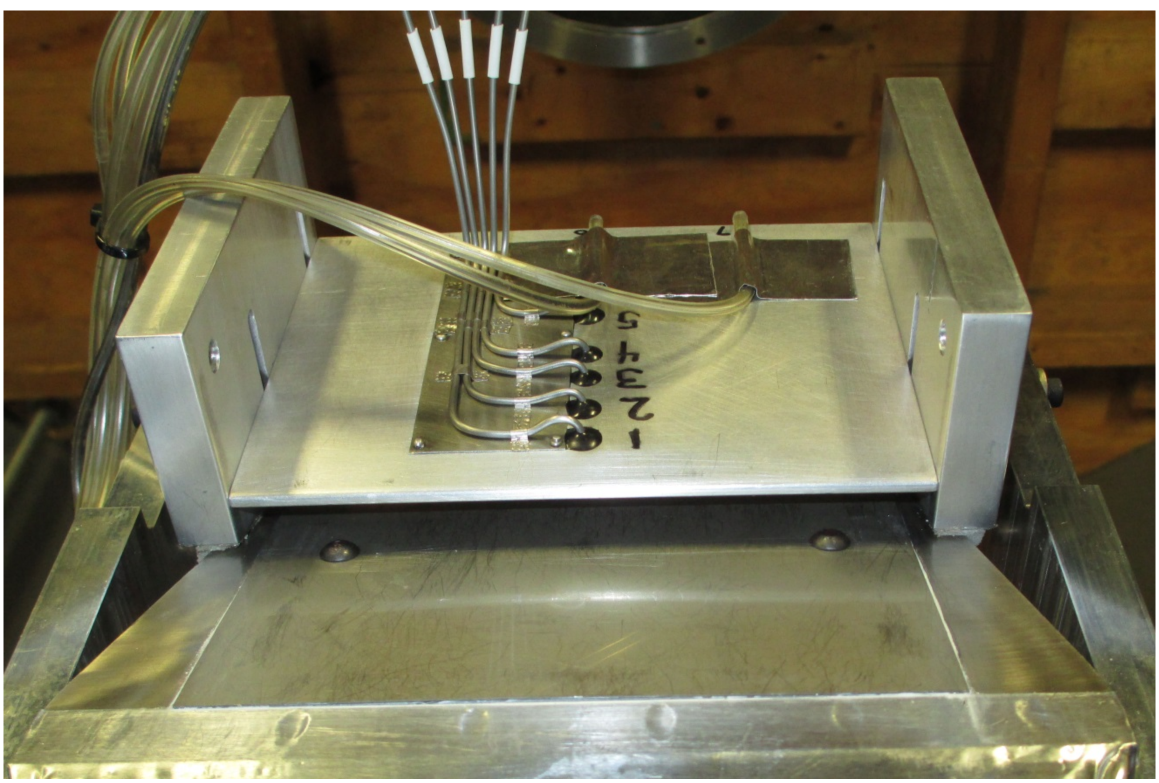

Config 3 – Larger slot and exit areas: view of ejector entry slot.

FIGURE 9g. MODEL PHOTOGRAPHS

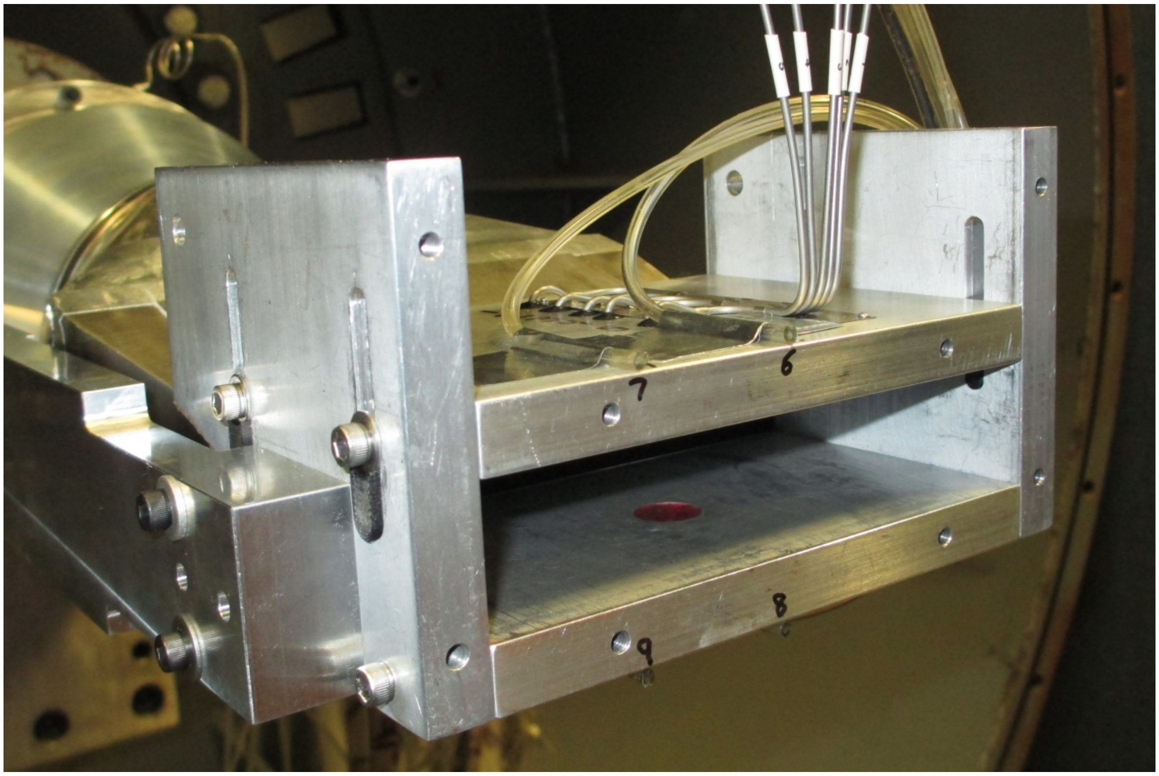

Config 3 – Larger slot and exit areas: view of ejector box exit.

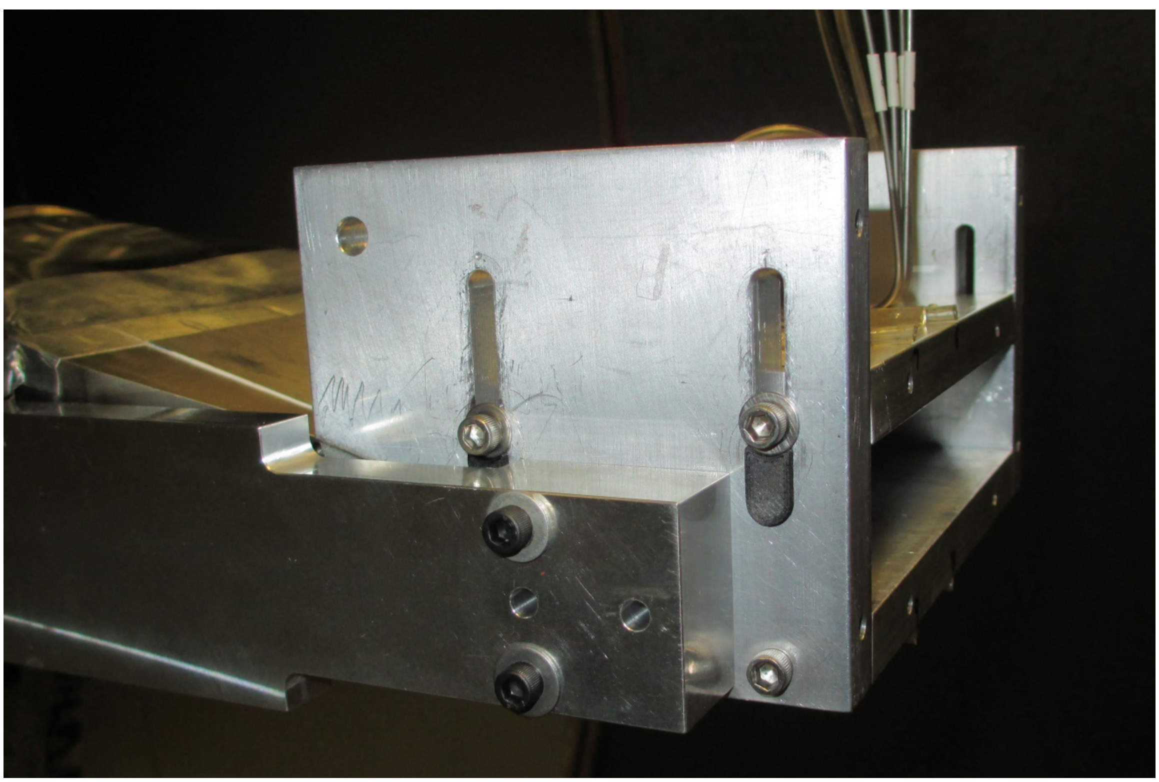

Config 4 – Divergent upper plate: view of ejector box.

FIGURE 9h. MODEL PHOTOGRAPHS

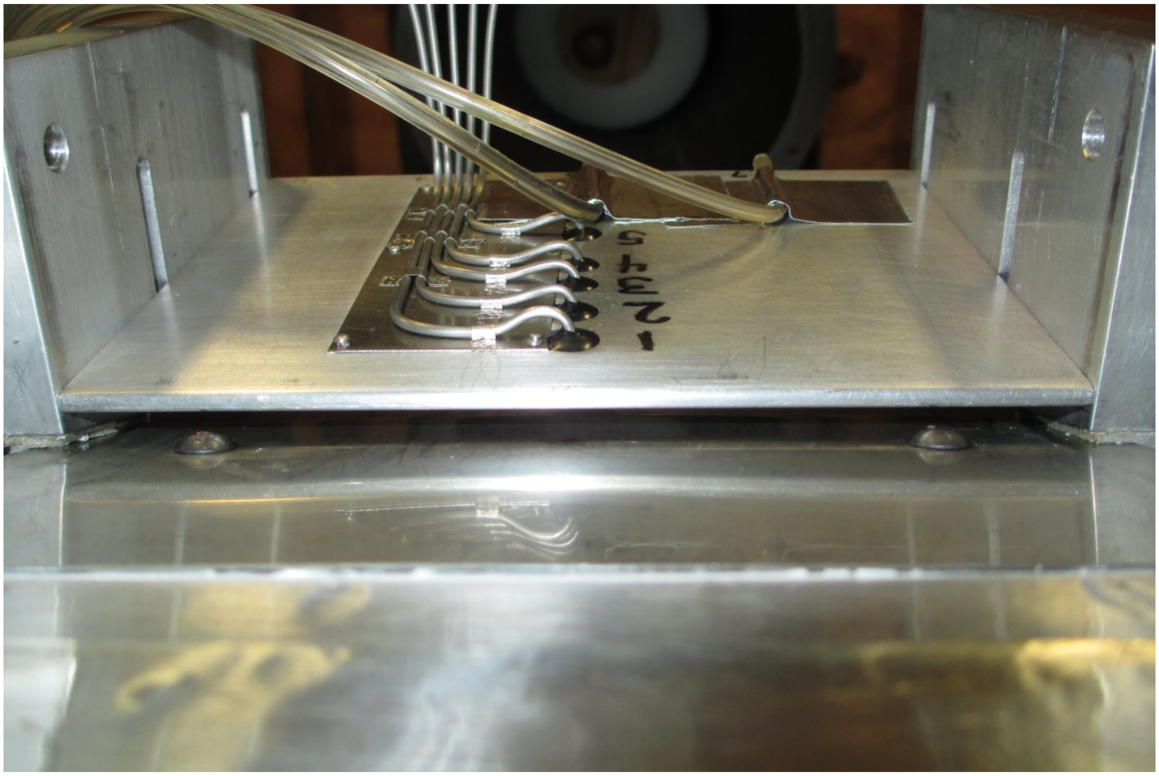

Config 4 – Divergent upper plate: view of ejector entry slot.

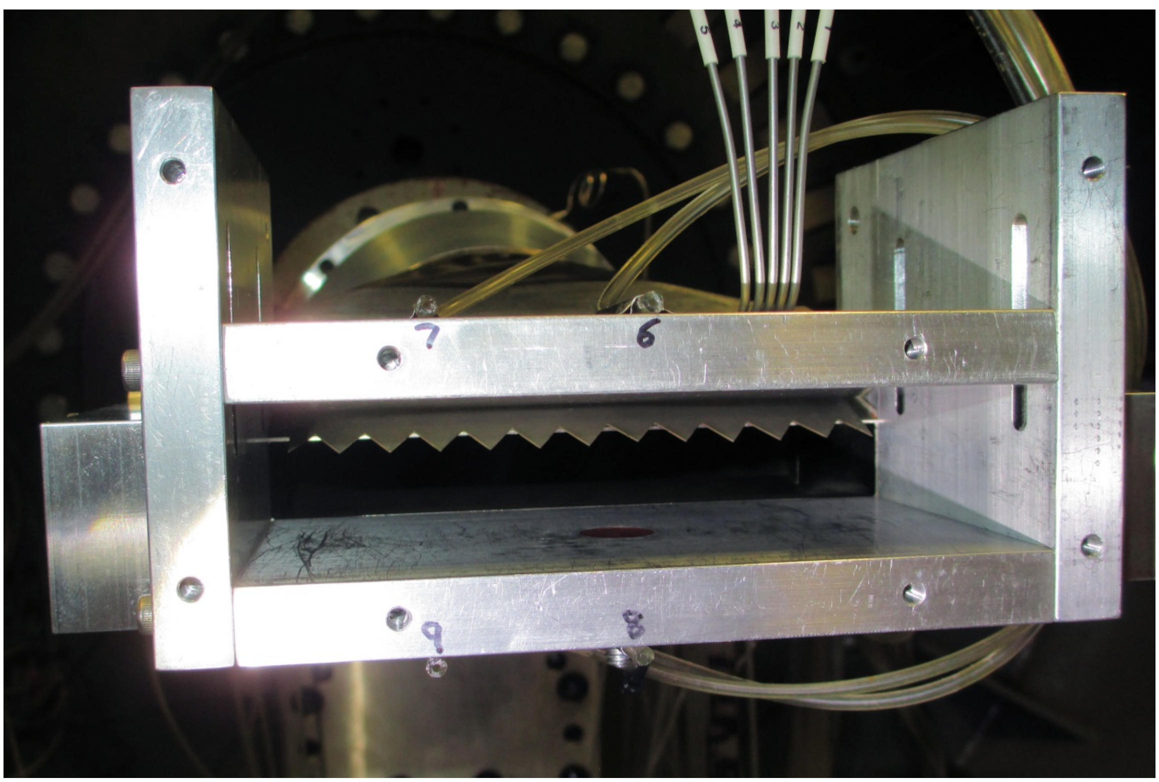

Config 4 – Divergent upper plate: view of ejector box exit.

FIGURE 9i. MODEL PHOTOGRAPHS

Data Point	λ_8	P_{t8} (psia)	T_{t8} (deg F)	P_{amb} (psia)	T_{amb} (deg F)	W_8 (lbm/sec)	C_{Tr}	C_{Tx}	C_{D8}	α (degrees)	Ly, Δr (inches)
Configuration 1 - Baseline with no tab strip											
1.02	3.001	42.008	71.877	13.999	68.577	3.3701	0.9815	0.9815	0.9813	0.07	-0.25
2.02	2.502	35.026	71.546	14.001	68.536	2.8083	0.9930	0.9928	0.9806	1.07	-0.29
3.02	2.107	29.499	71.625	14.001	68.139	2.3618	0.9938	0.9938	0.9794	0.19	-0.29
4.02	1.904	26.659	71.685	14.001	67.824	2.1320	0.9923	0.9923	0.9784	0.13	-0.28
5.02	1.707	23.902	71.715	13.999	67.850	1.8989	0.9904	0.9904	0.9792	0.29	-0.28
6.02	1.403	19.634	71.566	13.999	67.791	1.4540	0.9852	0.9852	0.9838	0.66	-0.25
Configuration 2 - Baseline with tab strip installed											
7.01	3.000	42.667	69.416	14.221	66.742	3.4321	0.9692	0.9692	0.9815	0.55	-0.25
8.02	2.503	35.595	66.480	14.223	66.163	2.8677	0.9748	0.9748	0.9805	0.09	-0.25
9.01*	2.103	29.906	68.845	14.219	64.893	2.3997	0.9804	0.9802	0.9790	-1.18	-0.21
9.02	2.104	29.919	66.195	14.222	65.492	2.4067	0.9809	0.9807	0.9789	-1.20	-0.25
10.02	1.903	27.062	65.772	14.224	64.719	2.1748	0.9859	0.9858	0.9777	0.37	-0.24
11.02	1.696	24.115	65.371	14.222	64.505	1.9175	0.9840	0.9840	0.9752	0.46	-0.25
12.02	1.400	19.921	65.308	14.225	64.589	1.4601	0.9784	0.9783	0.9689	0.58	-0.23
Configuration 3 - Larger slot and exit areas with tab strip installed											
13.01	2.996	42.630	65.312	14.229	67.364	3.4421	0.9764	0.9764	0.9814	0.28	-0.23
14.01	2.502	35.595	64.909	14.230	66.940	2.8721	0.9851	0.9844	0.9806	-2.22	-0.21
15.01	2.104	29.934	64.439	14.229	66.140	2.4139	0.9919	0.9919	0.9797	0.48	-0.22
16.01	1.907	27.129	63.920	14.229	65.889	2.1834	0.9904	0.9903	0.9774	0.64	-0.20
17.01	1.695	24.113	63.612	14.229	65.711	1.9197	0.9888	0.9888	0.9749	0.75	-0.21
18.01	1.403	19.956	63.522	14.229	65.499	1.4600	0.9830	0.9829	0.9645	0.91	-0.19
Configuration 4 - Divergent upper plate with tab strip installed											
19.02	2.992	42.566	65.033	14.226	65.246	3.4421	0.9467	0.9467	0.9826	0.07	-0.25
20.02	2.504	35.622	64.935	14.226	63.793	2.8780	0.9454	0.9393	0.9819	6.49	-0.08
21.02	2.105	29.950	64.700	14.227	64.096	2.4175	0.9146	0.9145	0.9809	0.38	-0.30
22.01	1.907	27.126	65.743	14.224	62.718	2.1857	0.8937	0.8937	0.9802	0.19	-0.27
23.02	1.705	24.249	63.942	14.225	63.114	1.9553	0.9364	0.9361	0.9867	1.43	-0.30
24.02	1.399	19.906	63.593	14.226	63.269	1.5322	0.9421	0.9417	1.0164	1.72	-0.27

***No Charge Data Points**

FIGURE 10. TABULATION OF MAJOR MODEL TEST RESULTS

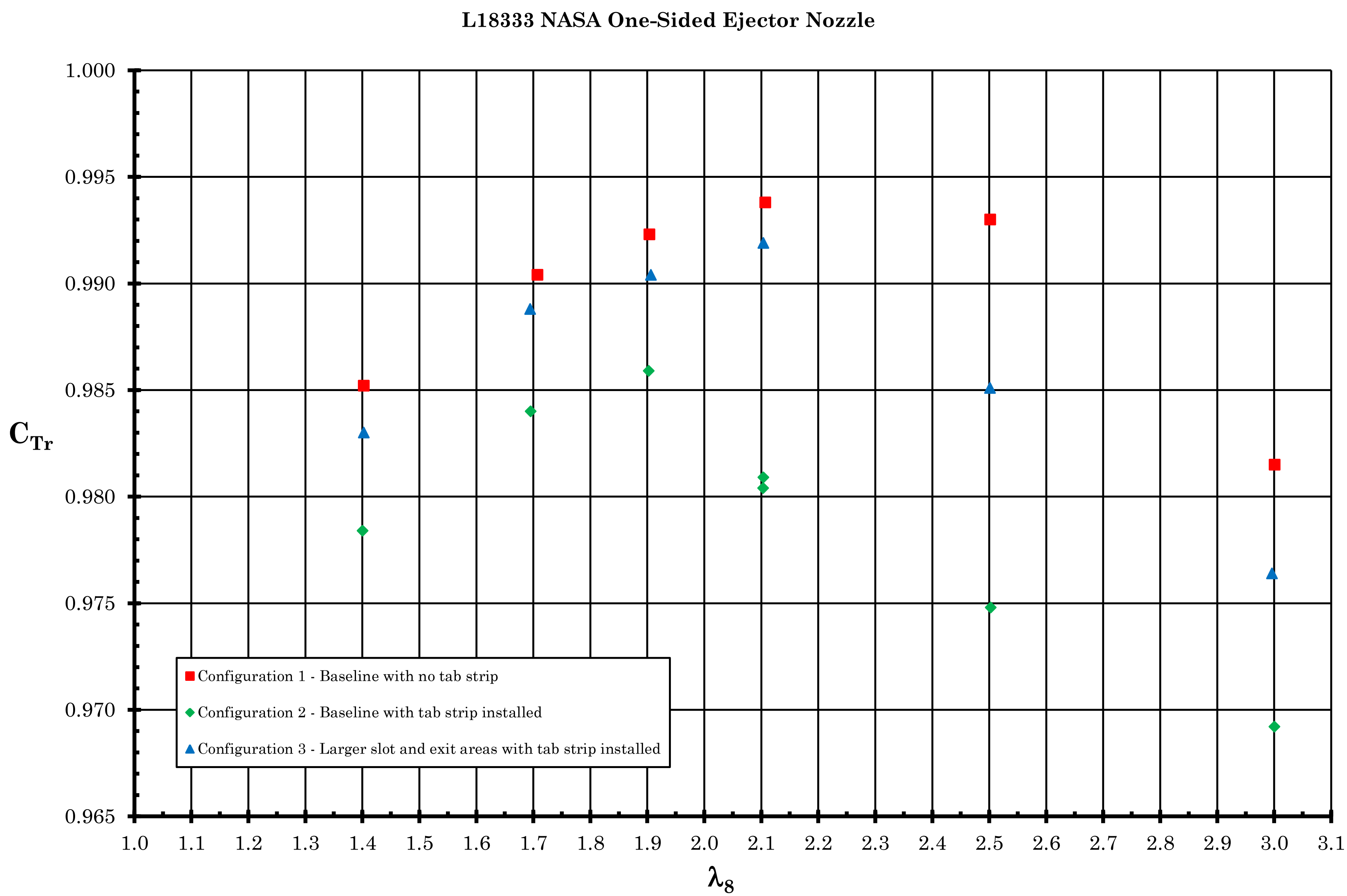

FIGURE 11a. NOZZLE THRUST COEFFICIENTS

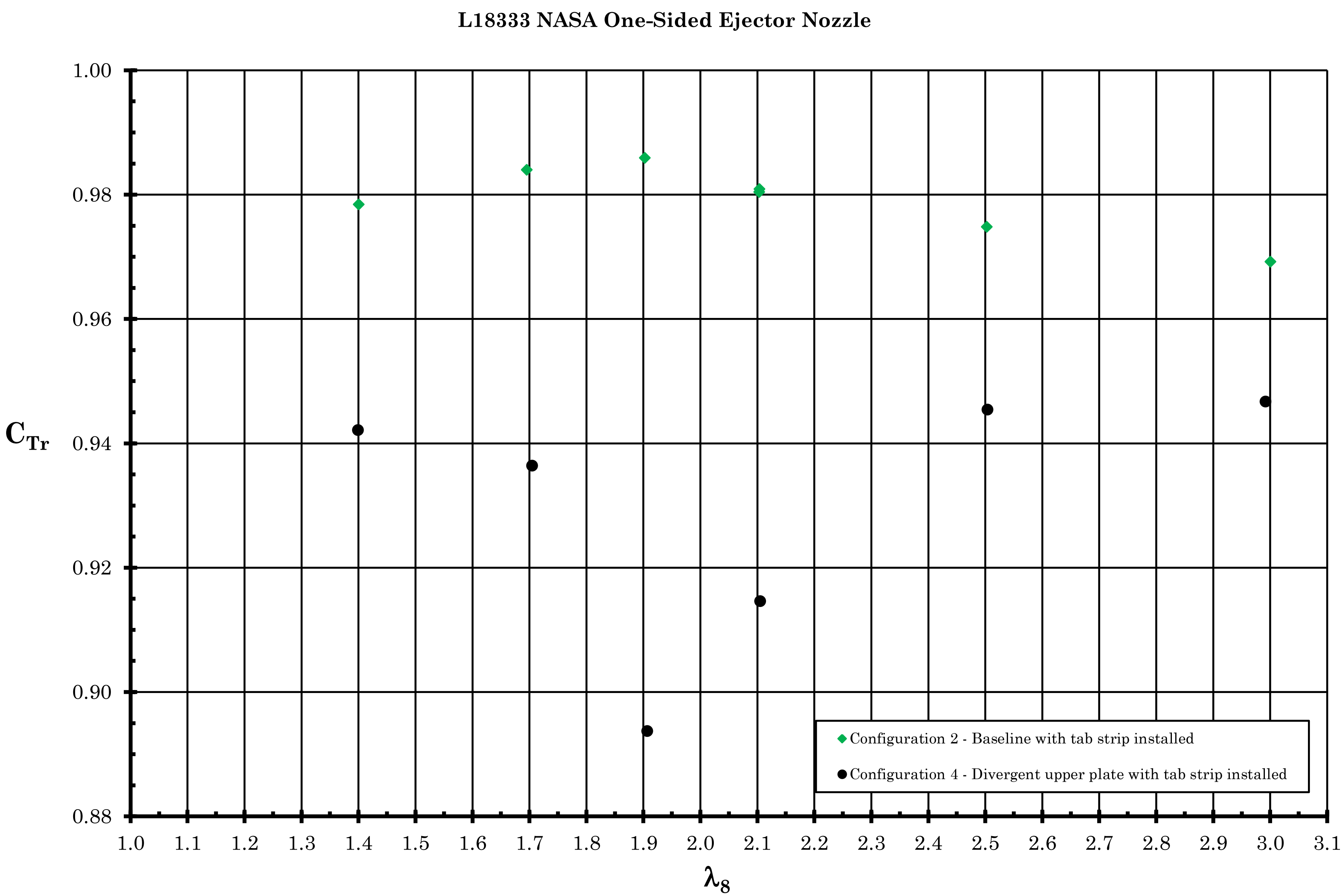

FIGURE 11b. NOZZLE THRUST COEFFICIENTS

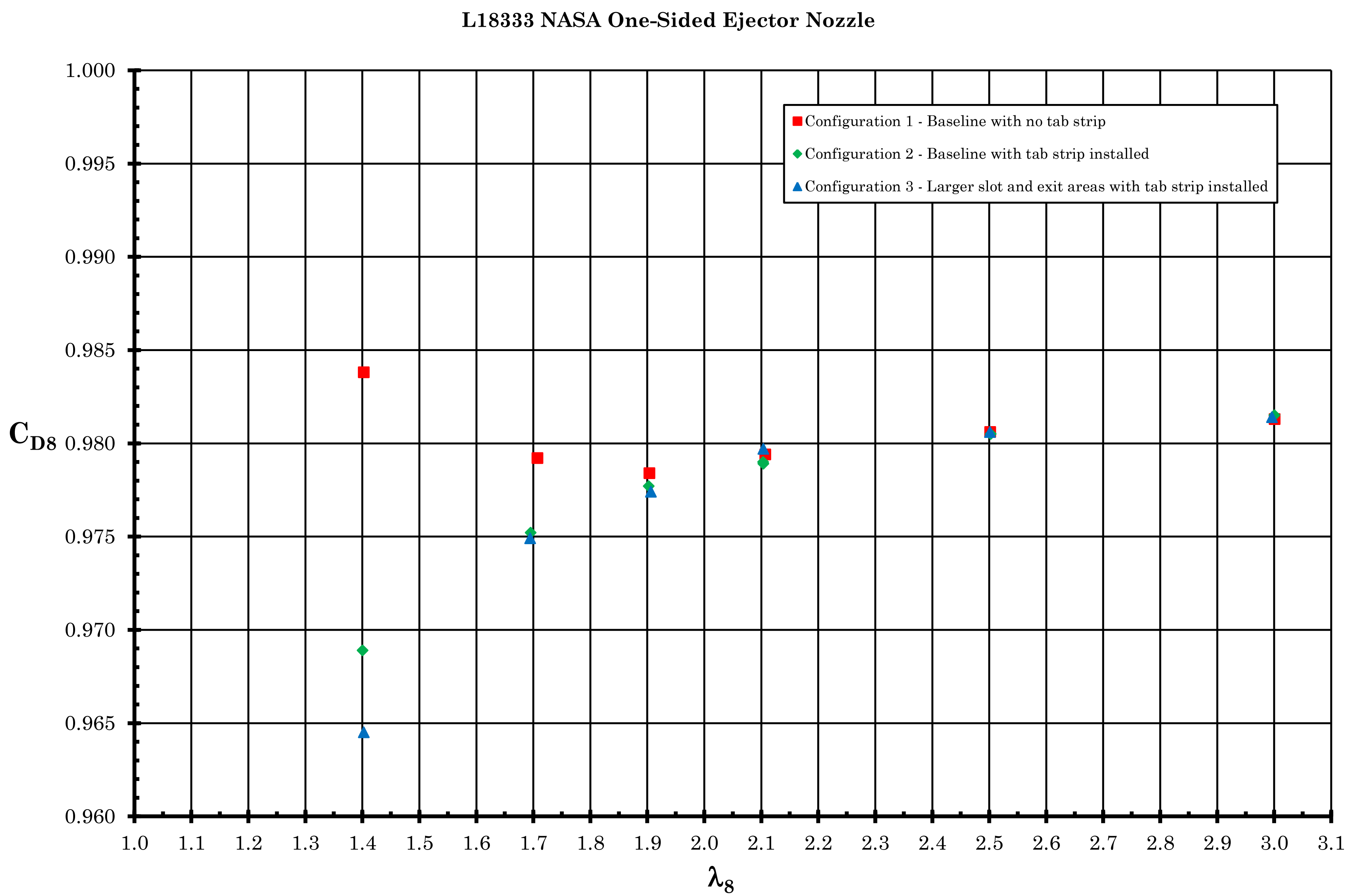

FIGURE 12a. NOZZLE DISCHARGE COEFFICIENTS

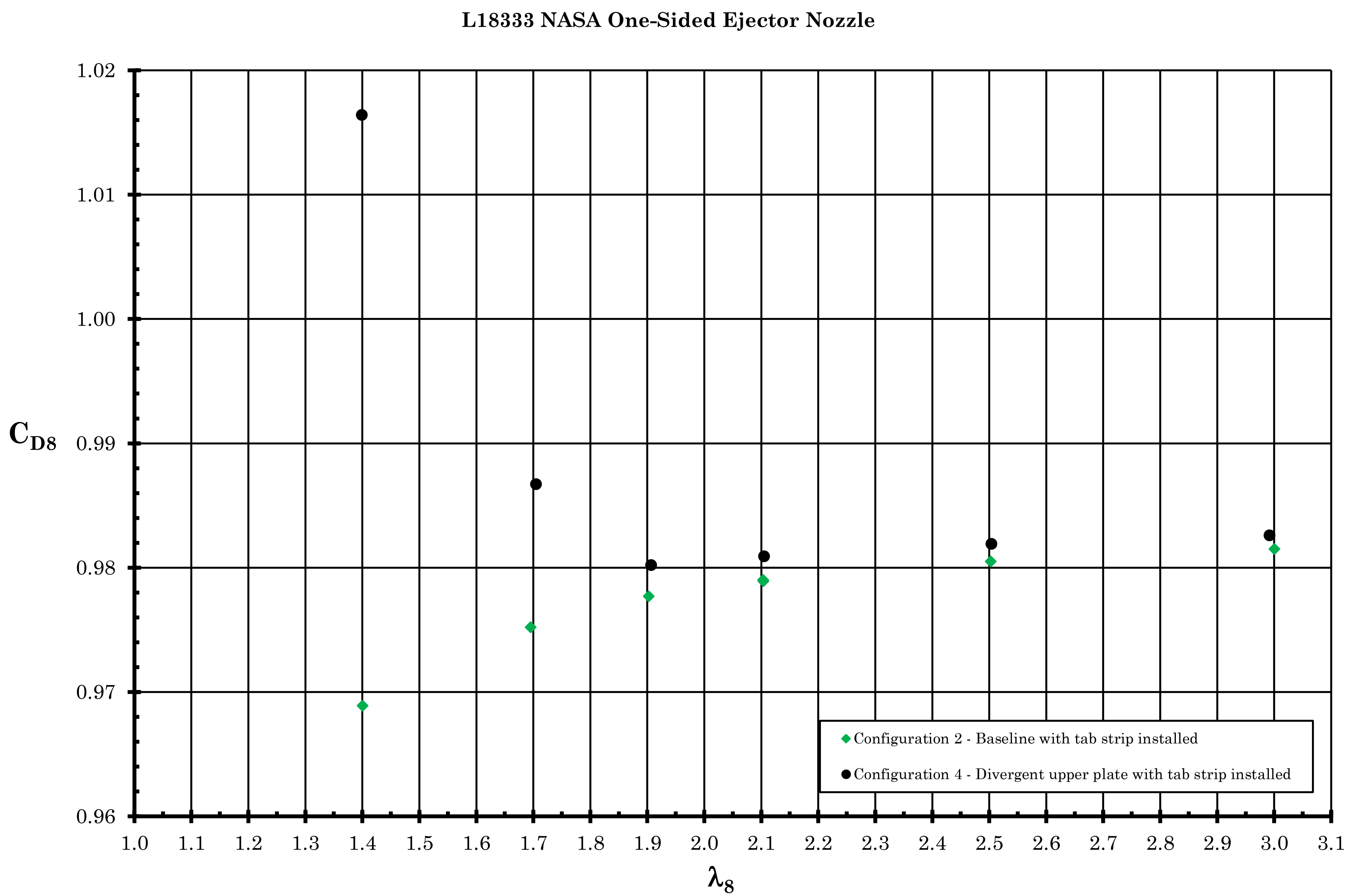

FIGURE 12b. NOZZLE DISCHARGE COEFFICIENTS

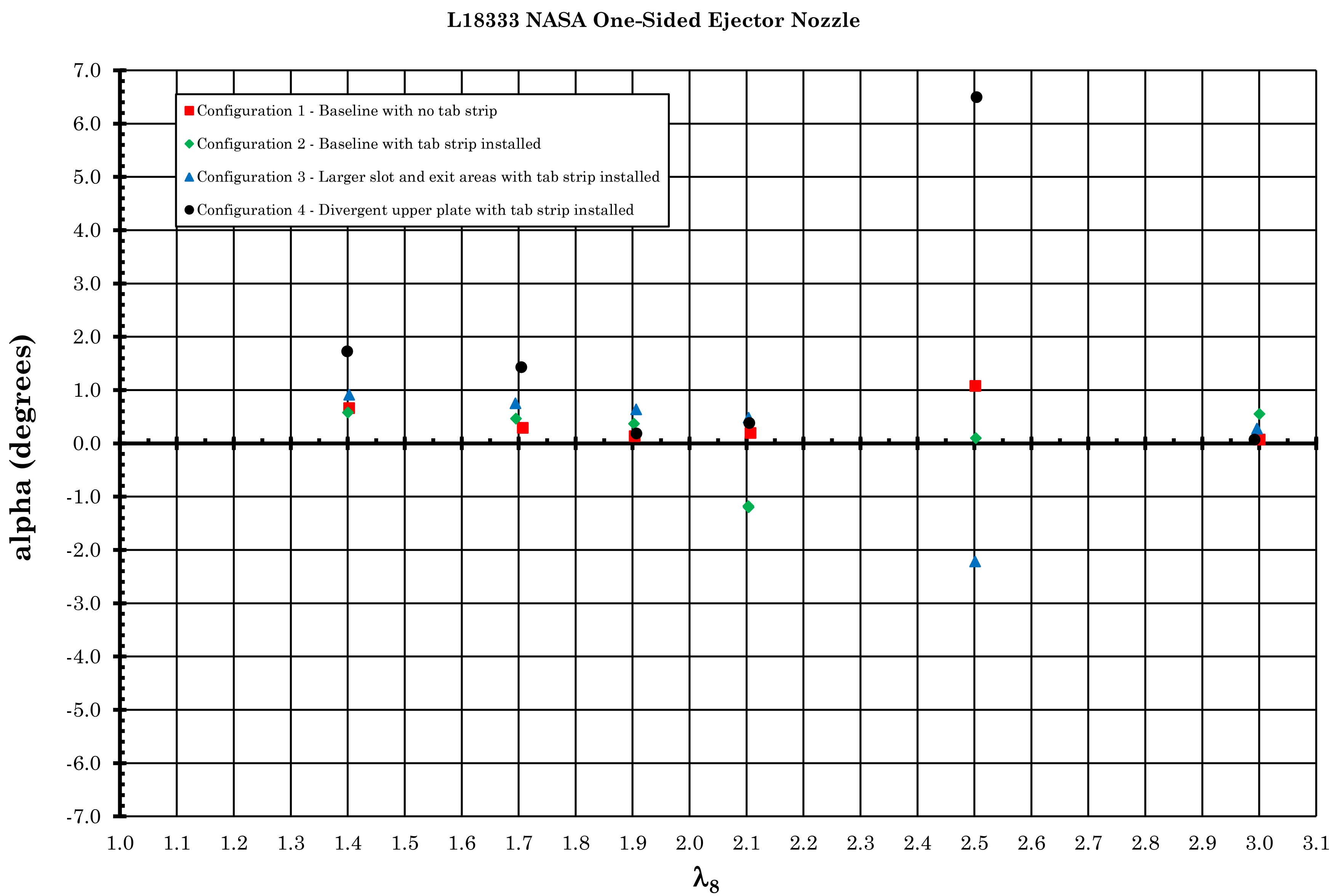

FIGURE 13. THRUST VECTOR ANGLES

JOB L18333 - NASA ONE-SIDED EJECTOR NOZZLE
ASE Detailed Drawing List

DRAWING NUMBER	REV.	TITLE
L18333-010	A	Model Assembly - NASA Ejector Test
L18333-100	A	Facility Adapter
L18333-101	-	Bracket - Ejector Nozzle Support
L18333-102	-	Ejector Box Modification
6070-079	D	6.5 inch Dia ID ASME Spacer Spool

For the hardware provided by NASA, part numbers were not specified and drawings were not provided.

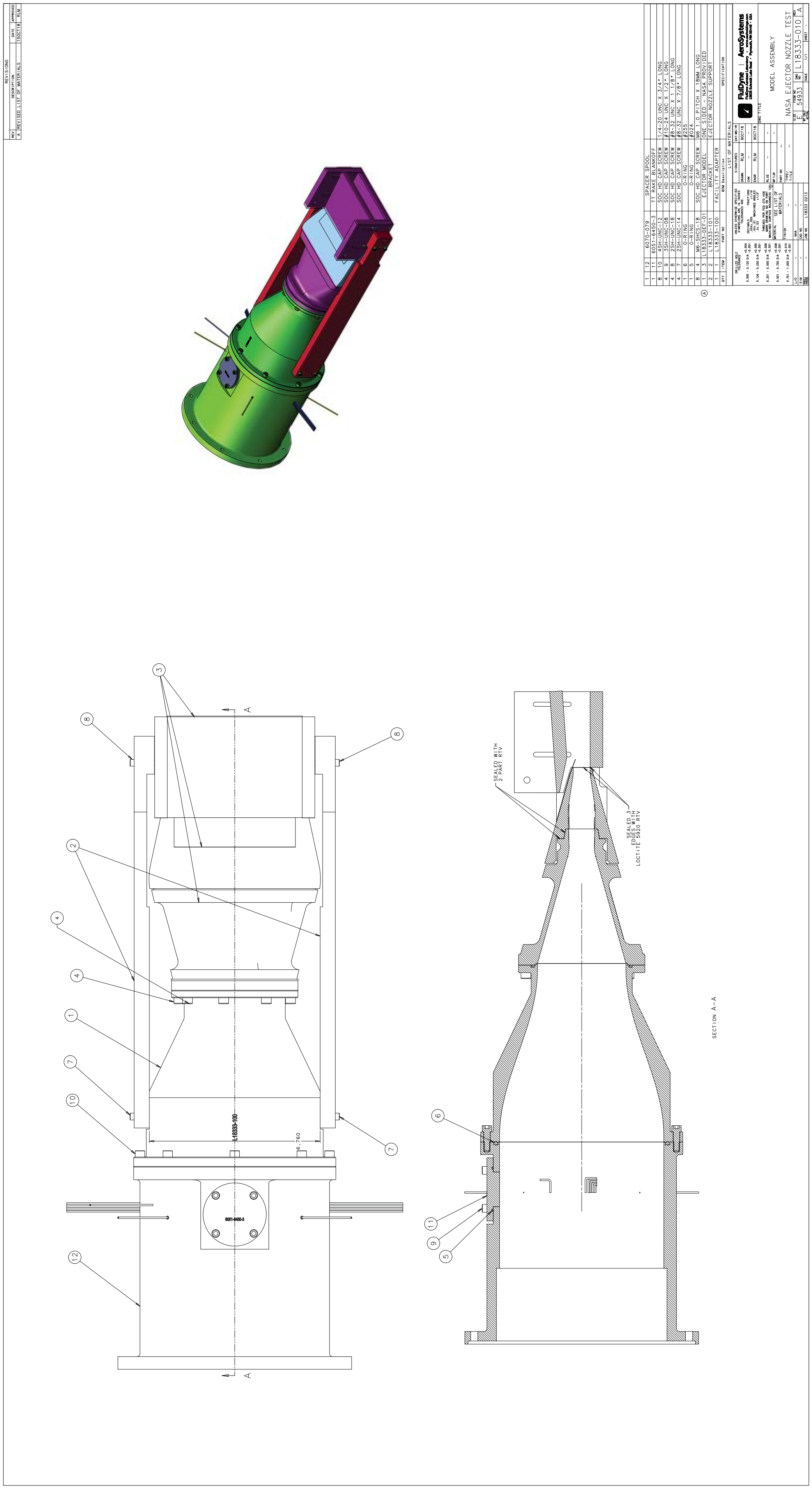

REVISIONS
REV
DESCRIPTION
DATE
APPROVED
A
REVISED LIST OF MATERIALS
10OCT18
RLM
QTY
ITEM
PART NO
BOM Description
SPECIFICATION
1 12 6070-079 SPACER SPOOL
1 11 6051-6450-3 TT RAKE BLANKOFF
8 10 4SH-UNC-12 SOC HD CAP SCREW 1/4-20 UNC X 3/4" LONG
4 9 3SH-UNC-08 SOC HD CAP SCREW #10-24 UNC X 1/2" LONG
4 8 2SH-UNC-18 SOC HD CAP SCREW #8-32 UNC X 1 1/8" LONG
4 7 2SH-UNC-14 SOC HD CAP SCREW #8-32 UNC X 7/8" LONG
1 6 O-RING O-RING #255
1 5 O-RING O-RING #024
8 4 M6-SHCS-18 SOC HD CAP SCREW M6 1.0 PITCH X 18MM LONG
1 3 L18333-DEF-01 EJECTOR MODEL ONE SIDED - NASA PROVIDED
2 2 L18333-101 BRACKET EJECTOR NOZZLE SUPPORT
1 1 L18333-100 FACILITY ADAPTER
LIST OF MATERIALS
FluiDyne | AeroSystems
MODEL ASSEMBLY
NASA EJECTOR NOZZLE TEST
SIZE E
FSCM NO 54933
DWG NO L18333-010
REV A
SCALE 1/1
SEALED WITH 2 PART RTV
SEALED 3 EDGES WITH LOCTITE 5920 RTV
L18333-100
6051-6450-3
6.760
SECTION A-A

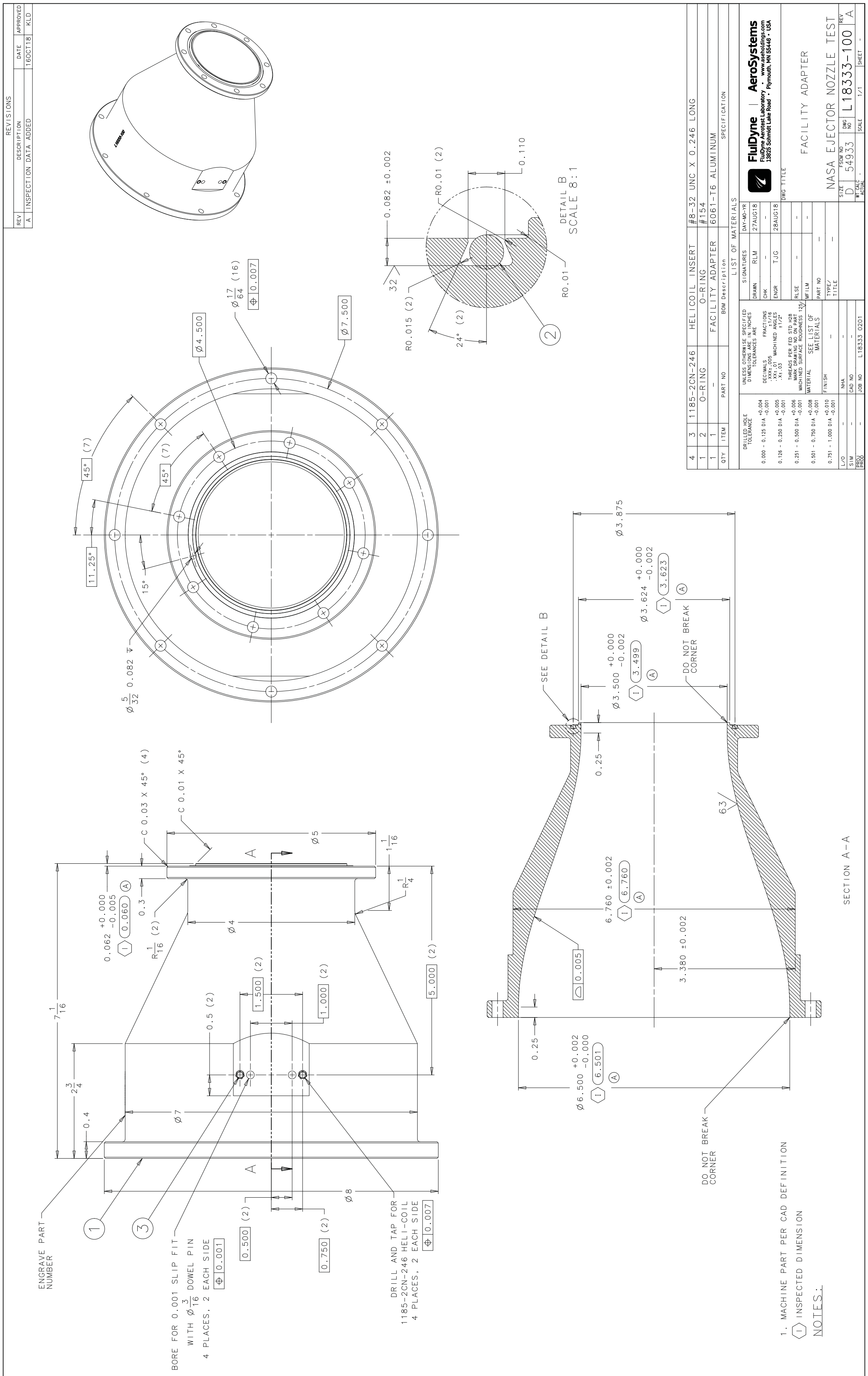
REVISIONS
REV A INSPECTION DATA ADDED 16OCT18 KLD
ENGRAVE PART NUMBER
BORE FOR 0.001 SLIP FIT WITH Ø3/16 DOWEL PIN 4 PLACES, 2 EACH SIDE
DRILL AND TAP FOR 1185-2CN-246 HELI-COIL 4 PLACES, 2 EACH SIDE
C 0.03 X 45° (4)
C 0.01 X 45°
SEE DETAIL B
DO NOT BREAK CORNER
DETAIL B
SCALE 8:1
SECTION A-A
1. MACHINE PART PER CAD DEFINITION
INSPECTED DIMENSION
NOTES:
4 3 1185-2CN-246 HELICOIL INSERT #8-32 UNC X 0.246 LONG
1 2 O-RING O-RING #154
1 1 – FACILITY ADAPTER 6061-T6 ALUMINUM
QTY ITEM PART NO BOM Description SPECIFICATION
LIST OF MATERIALS
UNLESS OTHERWISE SPECIFIED DIMENSIONS ARE IN INCHES
DRAWN RLM 27AUG18
ENGR TJG 28AUG18
FluiDyne | AeroSystems
FluiDyne Aerotest Laboratory • www.aseholdings.com
13825 Schmidt Lake Road • Plymouth, MN 55446 • USA
FACILITY ADAPTER
NASA EJECTOR NOZZLE TEST
SIZE D FSCM NO 54933 DWG NO L18333-100 REV A
SCALE 1/1
JOB NO L18333 0201

REVISIONS			
REV	DESCRIPTION	DATE	APPROVED
A	-	-	-

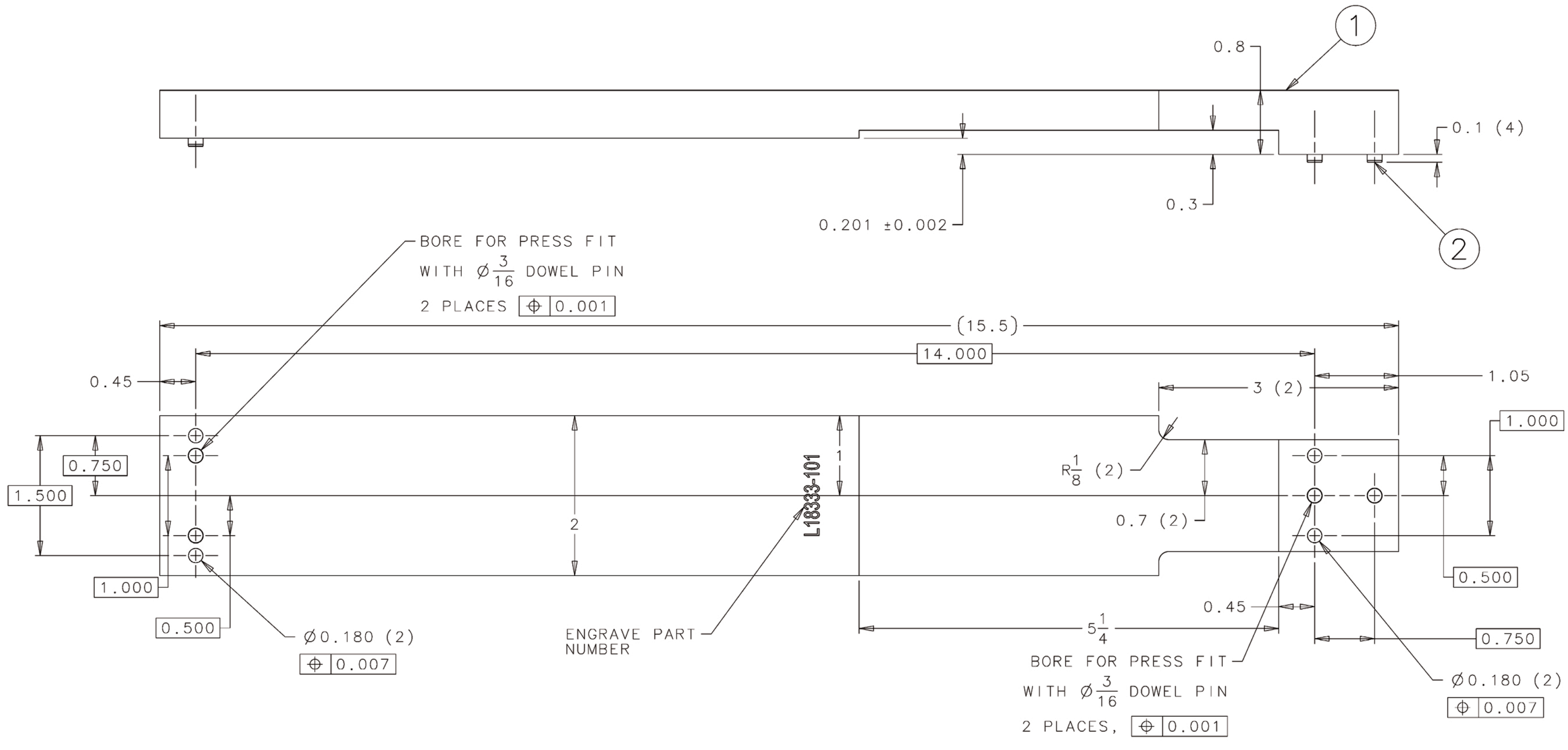

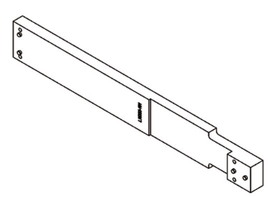

QTY	ITEM	PART NO	BOM Description	SPECIFICATION
4	2	3DP-06	DOWEL PIN	3/16 DIAMETER X 3/8" LONG, HARDENED
1	1	-	BRACKET	7075-T6 ALUMINUM

LIST OF MATERIALS

DRILLED HOLE TOLERANCE	
0.000 - 0.125 DIA	+0.004 -0.001
0.126 - 0.250 DIA	+0.005 -0.001
0.251 - 0.500 DIA	+0.006 -0.001
0.501 - 0.750 DIA	+0.008 -0.001
0.751 - 1.000 DIA	+0.010 -0.001
L/O	-
SIM	-
PROJ PROD	-

UNLESS OTHERWISE SPECIFIED DIMENSIONS ARE IN INCHES TOLERANCES ARE
DECIMALS .XXX± .005 .XX± .01 .X± .03
FRACTIONS ±1/16 MACHINED ANGLES ±1/2°
THREADS PER FED STD H28
MARK DRAWING NO ON PART
MACHINED SURFACE ROUGHNESS 125

MATERIAL	SEE LIST OF MATERIALS
FINISH	-
NHA	-
CAD NO	-
JOB NO	L18330 0201

SIGNATURES		DAY-MO-YR
DRAWN	RLM	27AUG18
CHK	-	-
ENGR	TJG	28AUG18
RLSE	-	-
MFILM		-
PART NO	—	
TYPE/ TITLE	—	

FluiDyne | AeroSystems
FluiDyne Aerotest Laboratory • www.aseholdings.com
13825 Schmidt Lake Road • Plymouth, MN 55446 • USA

DWG TITLE
BRACKET
EJECTOR NOZZLE SUPPORT
NASA EJECTOR NOZZLE TEST

SIZE	FSCM NO	DWG NO	REV
C	54933	L18333-101	–
WT CALC ACTUAL -		SCALE 1/1	SHEET -

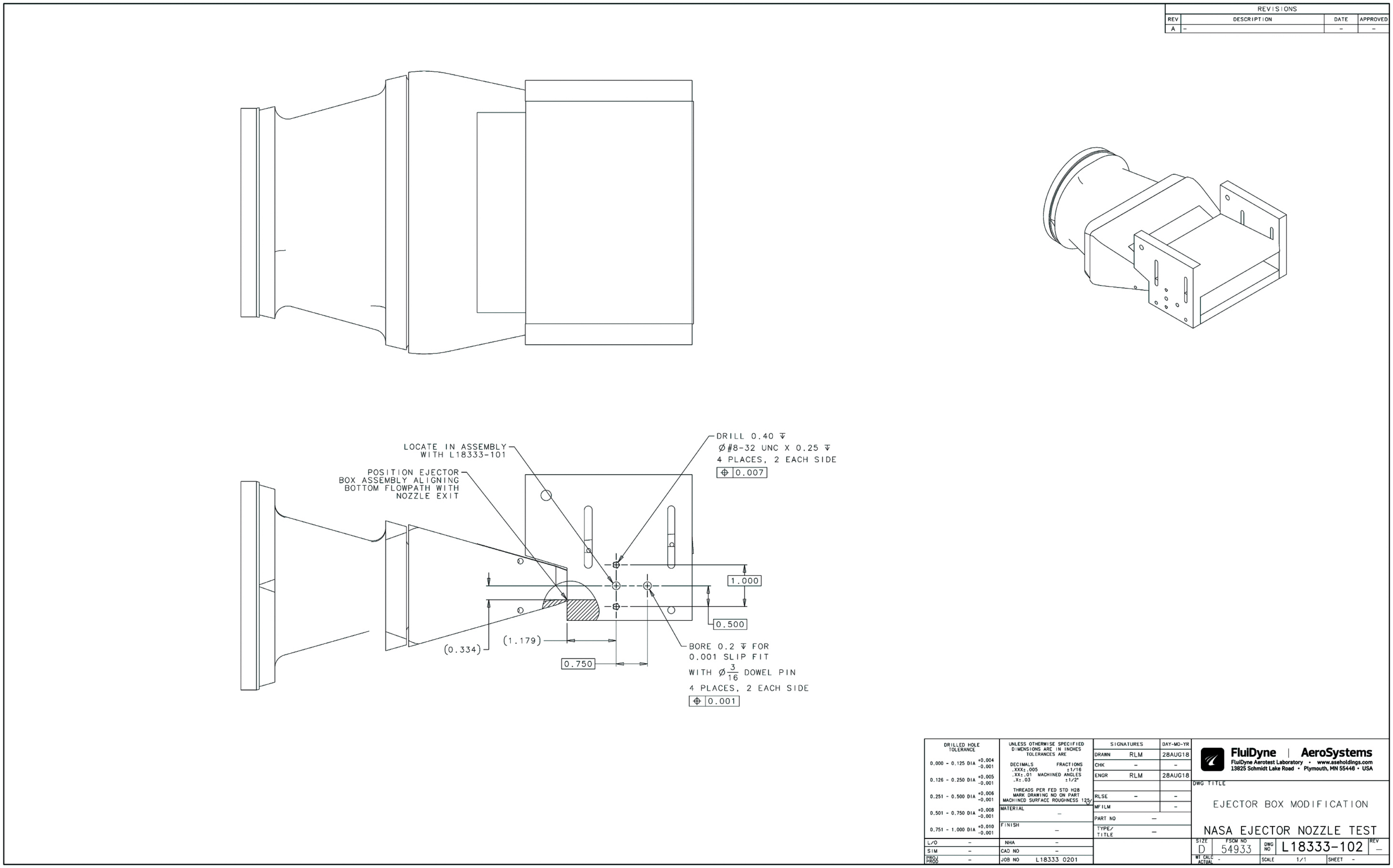

REVISIONS
REV | DESCRIPTION | DATE | APPROVED
A | - | - | -
LOCATE IN ASSEMBLY WITH L18333-101
POSITION EJECTOR BOX ASSEMBLY ALIGNING BOTTOM FLOWPATH WITH NOZZLE EXIT
DRILL 0.40 ↧
Ø #8-32 UNC X 0.25 ↧
4 PLACES, 2 EACH SIDE
⌖ 0.007
1.000
0.500
(1.179)
(0.334)
0.750
BORE 0.2 ↧ FOR 0.001 SLIP FIT
WITH Ø 3/16 DOWEL PIN
4 PLACES, 2 EACH SIDE
⌖ 0.001
DRILLED HOLE TOLERANCE
0.000 - 0.125 DIA +0.004 -0.001
0.126 - 0.250 DIA +0.005 -0.001
0.251 - 0.500 DIA +0.006 -0.001
0.501 - 0.750 DIA +0.008 -0.001
0.751 - 1.000 DIA +0.010 -0.001
UNLESS OTHERWISE SPECIFIED DIMENSIONS ARE IN INCHES TOLERANCES ARE
DECIMALS .XXX±.005 .XX±.01 .X±.03
FRACTIONS ±1/16 MACHINED ANGLES ±1/2°
THREADS PER FED STD H28
MARK DRAWING NO ON PART
MACHINED SURFACE ROUGHNESS 125
MATERIAL -
FINISH -
L/O -
SIM -
PROJ PROD -
NHA -
CAD NO -
JOB NO L18333 0201
SIGNATURES | DAY-MO-YR
DRAWN RLM 28AUG18
CHK - -
ENGR RLM 28AUG18
RLSE - -
MFLM -
PART NO -
TYPE/TITLE -
FluiDyne | AeroSystems
FluiDyne Aerotest Laboratory • www.aseholdings.com
13825 Schmidt Lake Road • Plymouth, MN 55446 • USA
DWG TITLE
EJECTOR BOX MODIFICATION
NASA EJECTOR NOZZLE TEST
SIZE D
FSCM NO 54933
DWG NO L18333-102
REV -
WT CALC ACTUAL -
SCALE 1/1
SHEET -

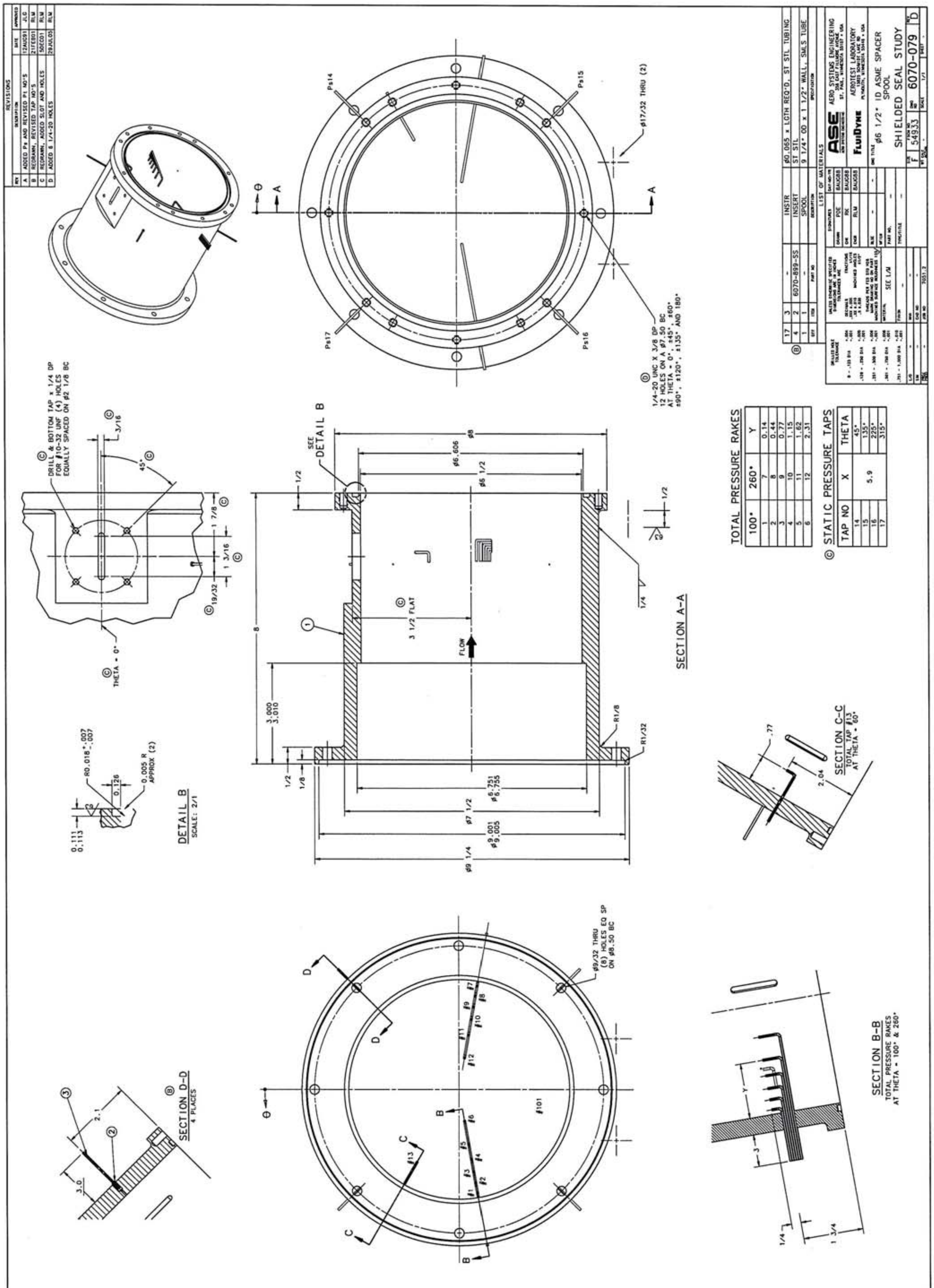
SECTION A-A
SECTION B-B
TOTAL PRESSURE RAKES AT THETA = 100° & 260°
SECTION C-C
TOTAL TAP #13 AT THETA = 60°
SECTION D-D
4 PLACES
DETAIL B
SCALE: 2/1
SEE DETAIL B
FLOW
TOTAL PRESSURE RAKES
STATIC PRESSURE TAPS
1/4-20 UNC X 3/8 DP
12 HOLES ON A ø7.50 BC
AT THETA = 0°, ±45°, ±60°
±90°, ±120°, ±135° AND 180°
ø17/32 THRU (2)
ø9/32 THRU
(8) HOLES EQ SP
ON ø8.50 BC
DRILL & BOTTOM TAP x 1/4 DP
FOR #10-32 UNF (4) HOLES
EQUALLY SPACED ON ø2 1/8 BC
THETA = 0°
3 1/2 FLAT
REVISIONS
LIST OF MATERIALS
AERO SYSTEMS ENGINEERING
AEROTEST LABORATORY
FLUIDYNE
ø6 1/2" ID ASME SPACER SPOOL
SHIELDED SEAL STUDY
6070-079